We sincerely appreciate your interest in our paper. As you have pointed out, this study aims to significantly contribute to determining the reliability of GCMs in climate predictions and impact assessments. Previous bias correction studies have primarily focused on selecting appropriate methods based on performance. However, this approach has limitations due to the uncertainties arising from various factors. Our study suggested a Comprehensive Index that integrates uncertainty quantification and performance evaluation in selecting bias correction methods. This approach provides an opportunity to further enhance the reliability of climate models. Specifically, the results of this study are expected to be effectively utilized in future processes for selecting GCMs and evaluating various methods applied to models, facilitating the selection of the most suitable approaches. Once again, we sincerely appreciate your interest in and valuable feedback. We will now begin addressing your questions.

Comment 1

Why was only the historical period used? If there is a specific reason, it must be clearly stated.

Answer

This study used the three quantile mapping methods by dividing the historical period into training and validation periods. This approach has two main reasons. First, this study divided the historical period into two periods to analyze the performance and uncertainty during the validation period. This concept can intuitively evaluate how precipitation corrected by bias correction methods can be projected into the future. Specifically, the historical period allows for direct comparison with reliable observational data such as ERA5, providing a robust basis to accurately assess the differences between bias-corrected GCM outputs and observed data. This approach facilitates a comparison of the bias correction performance of QDM, EQM, and DQM. Furthermore, using historical data helps remove uncertainties associated with future simulations, enabling the study to focus solely on the performance differences of the correction methods. This was a critical reason to enhance the reliability of the research.

Second, future climate projections are subject to additional uncertainties arising from factors such as GHG emission scenarios and structural differences among GCMs. These factors can hinder the evaluation of the bias correction methods themselves. By using only the historical period, this study concentrated on verifying and comparing the inherent performance of the correction methods, aligning with the study's objectives.

We have added the following sentences to Section 2.3 Quantile Mapping to clarify this.

This study divided the data into a training period (1980-1996) and a validation period (1997-2014) to correct the historical period's data. This approach minimizes the influence of uncertainties associated with future projections, allowing the study to focus on evaluating the intrinsic performance differences

of the QM methods.

Comment 2

Developing a comprehensive index is a significant strength of this study. However, there is insufficient explanation of the differences from previous methods to highlight its originality. Please address this. Additionally, the comprehensive index appears to be overly limited. Such a restrictive methodology may reduce the efficiency of the approach, which warrants further discussion.

Answer

Thank you for your valuable comment. We have revised the manuscript to clarify further the originality of the comprehensive index proposed in this study and highlight its differences from previous methods. Unlike earlier studies, which primarily focused on the performance of bias correction methods, this study introduces a CI that considers both performance and uncertainty simultaneously. This consideration is a significant advancement, allowing for a more comprehensive and balanced evaluation of bias correction methods. By integrating uncertainty into the evaluation process, the CI addresses a critical limitation of traditional performance-centered approaches, enhancing the reliability and robustness of method selection for climate change research. Additionally, in response to concerns that CI may be seen as overly restrictive, the methodology details that incorporating uncertainty along with performance allows the approach to be leveraged by a variety of factors. The added discussion can explain why this comprehensive evaluation framework is essential for making well-informed decisions regarding climate projections.

The discussion section explains the strengths of CI:

Unlike previous studies that focused on the performance of bias correction methods (Song et al., 2024a; Teutschbein and Seibert, 2012; Smitha et al., 2018), this study suggests a CI that integrates the performance and uncertainty metrics. This approach enhances the robustness of bias correction method selection and provides a more holistic evaluation framework.

The additional reference included in this study is as follows:

Smitha, P.S., Narasimhan, B., Sudheer, K.P., and Annamalai, H.: An improved bias correction method of daily rainfall data using a sliding window technique for climate change impact assessment. J. Hydrol. 556, 100–118. https://doi.org/10.1016/j.jhydrol.2017.11.010, 2018.

In response to your concerns, we have revised the methodology section to address the flexibility of the CI framework. Specifically, the following sentence has been added to highlight the adaptability of performance and uncertainty metrics:

Additionally, the methodology offers flexibility in selecting performance and uncertainty metrics. Alternative MCDA methods beyond TOPSIS can be utilized for performance indicators, or indices that effectively represent the model's performance can be employed to calculate the CI. Similarly, for uncertainty indicators, approaches such as variance, standard deviation, or other uncertainty quantification techniques can be applied to enhance the robustness of the framework further.

Comment 3

DQM performs worse overall compared to other methods. The reasons for this must be explained. However, as QM methods are not newly proposed in this study but adopted from existing ones, it is unnecessary to deeply analyze the cause (this could be a topic for a future study). A brief explanation in the context of specific climate phenomena should suffice.

Answer

Thank you for pointing out the need to explain why DQM performs worse than other methods. Based on the discussion section, DQM's performance can be attributed to its limitations in handling nonlinear climate patterns and extreme events. DQM effectively corrects the meaning through its detrending process. It does not sufficiently account for all quantiles in the precipitation distribution, particularly extremes. This limitation increases uncertainty, especially in regions with complex climate conditions like Southeast Asia, East Africa, and the Alps in Europe. These findings are consistent with previous studies, highlighting DQM's difficulty in accurately capturing long-term climate trends and variability (Berg et al., 2022; Cannon et al., 2015). In response to your comment, the following paragraph is included in the discussion section of the manuscript:

DQM showed the highest weight variance across all continents, indicating more significant uncertainty when applied to various GCMs. This uncertainty was particularly pronounced in regions with complex climate conditions, such as Southeast Asia, East Africa, and the Alps in Europe. These results align with Berg et al. (2022), who highlighted DQM's limitations in capturing long-term climate trends and extreme events. The higher uncertainty associated with DQM suggests that, while its detrending process is effective in correcting the mean, it may struggle in regions dominated by nonlinear climate patterns, as it does not sufficiently account for all quantiles in the distribution, particularly extremes, as noted by Cannon et al. (2015).

Comment 4

The authors used entropy as a criterion weight for TOPSIS. Is there a reason for this choice? Since MCDA is widely used in other fields, incorporating more complex weights might be more appropriate.

Answer

Thank you for your comment regarding using entropy to determine the criterion weights in TOPSIS. The reason for selecting entropy is to assign objective weights based on the data. Entropy weights reflect the variability and distribution of each criterion within the dataset, minimizing subjectivity in the weighting process. This ensures that the calculated weights are determined solely by the data, which is crucial for studies comparing bias correction methods across diverse and complex regions.

We have added the following sentence to the methodology section in response to your comment.

This study used entropy theory to calculate the weights for each criterion. Entropy weighting ensures sufficient objectivity by calculating weights based on the variability and distribution of data. This approach minimizes subjectivity, preventing biases in the weighting process.

While we acknowledge that more intricate weighting schemes, such as expert judgment or hybrid approaches, could integrate additional perspectives, our objective was to establish a straightforward, generalized framework to apply without requiring domain-specific expertise. The simplicity and scalability of entropy weighting make it a suitable choice for determining weights.

Comment 5

Model performance can vary significantly depending on the climate zone, but in most cases, the performance is reported to be very high (e.g., EVS: 0.98 (DQM)). Such results indicate exceptional performance. This should be mentioned in the Discussion section.

Answer

Thank you for your comment. The three QM methods were undoubtedly closer to ERA5 compared to the raw GCMs. Additionally, their performance is fine for applications in various fields; they demonstrate high performance. In response to your comments, we have added the following paragraph to the Discussion section.

Of course, the three QM methods showed high performance across most continents, effectively correcting the biases in daily precipitation from GCMs. However, the corrected daily precipitation varies subtly among the three methods, with these differences becoming more pronounced in extreme events or specific evaluation metrics.

Comment 6

Why was only ERA5 selected for comparison? It may not pose a significant issue without a valid reason, but considering multiple reference datasets is essential for evaluating performance.

Answer

Thank you for your comment. ERA5, produced by the European Centre for Medium-Range Weather

Forecasts (ECMWF), provides high-resolution reanalysis data applicable on a global scale and has been widely used for evaluating the performance of climate models. ERA5's consistent methodology, high temporal and spatial resolution, and comprehensive assimilation of observational data make it highly suitable for assessing the performance of bias correction methods. Furthermore, ERA5 is frequently adopted in high-impact journals ranked in Q1 or above to emphasize the reliability of analyses.

https://doi.org/10.1029/2024EF004541

This study used ERA5 reanalysis data to contextualize the 2021 heatwave within historical records, covering the period from 1950 to 2022.

https://doi.org/10.1029/2021EF002625

In the study, ERA5 reanalysis data were employed to evaluate the performance of CMIP6 models in simulating historical climate conditions.

https://doi.org/10.5194/gmd-17-191-2024

This study used ERA5 data to evaluate the performance of downscaled climate projections by comparing them against historical reanalysis data.

https://doi.org/10.5194/gmd-17-8665-2024

In the study, ERA5 data were employed as a reference to assess the performance of downscaled climate products. This application of ERA5 data underscores its credibility and widespread acceptance in high-impact climate research, reinforcing our decision to use ERA5 as the reference dataset in our study.

We added the following statement to the methodology to justify the use of ERA5 as reference data:

ERA5 has been widely used in various studies to ensure reliability of climate model evaluation and climate change assessment (Jeong et al., 2024; Virgilio et al., 2024; Baek et al., 2024).

We have added the following references to the article:

Jeong, D.I., Yu, B., Cannon, A.J.: 2021 Heatwave Over Western North America: Structural Uncertainty and Internal Variability in GCM Projections of Humidex and Temperature Extremes. Earth's futur 12, 8, e2024EF004541. https://doi.org/10.1029/2024EF004541, 2024.

Virgilio, G.D., Tam, F.J.E., Nishant, N., Evans, J.P., Thomas, C., Riley, M.L., Beyer, K., Grose, M.R., Narsey, S., Delage, F.: Selecting CMIP6 GCMs for CORDEX Dynamical Downscaling: Model Performance, Independence, and Climate Change Signals. Earth's futur 10, 4, e2021EF002625. https://doi.org/10.1029/2021EF002625, 2024.

Baek, S.H., Ullrich, P.A., Dong, B., Lee, J.: Evaluating downscaled products with expected

hydroclimatic co-variances. Geosci. Model Dev. 17, 23, 8665–8681. https://doi.org/10.5194/gmd-17-8665-2024, 2024.

Comment 7

Why does DQM yield higher estimates for extreme precipitation? Could this be because DQM emphasizes variability in the data due to detrending?

Answer

Thank you for your comment. DQM is a bias correction method designed to correct discrepancies between GCMs and reference data and address long-term trends and variability in precipitation. Unlike other QM methods, DQM considers a detrending process that removes long-term trends from modeled data before applying bias correction. This method helps capture bias in extreme climate signals but can result in some discrepancies when comparing bias-corrected precipitation to observed values. DQM preserves the expected climate signals derived from GCM outputs, ensuring consistency with modeled trends. Nevertheless, DQM can overestimate extreme precipitation events compared to observations, as shown in the results of this study. This is because detrending in the correction process can amplify variability, leading to further overestimation in the tail of the precipitation distribution. Furthermore, this method has higher uncertainties in regions with nonlinear or complex climate patterns due to its sensitivity to variability and dependence on the detrending process. This study applied DQM to correct daily precipitation data for six continents using 11 CMIP6 GCMs. DQM effectively captured relative variability and produced results consistent with the predicted climate signal, but overestimated extreme precipitation values compared to observations, which were more frequent in countries and continents where extreme precipitation frequently occurred.

The following three factors may contribute to the overestimation of extreme precipitation corrected using DQM:

1. The detrending process emphasizes the relative variability of data, making DQM particularly sensitive to extreme values. If the model's extreme values are adjusted more significantly than the observed data, the distribution width in the extreme range may be amplified due to the detrending process.

2. DQM adjusts the model data by matching its cumulative distribution function to that of the reference data. However, if the model's distribution is broader than the observed data for extreme values, this mismatch may lead to overestimation. The emphasis on relative values through detrending can further expand the extremes during adjustment.

3. DQM restores the long-term mean to the corrected data as part of the process. This restoration may overestimate the relative contribution of extremes, mainly when the differences in mean and distribution

between the observed and modeled values are significant. The more pronounced these differences, the greater the potential overestimation of extremes.

We describe this issue of DQM-corrected extreme precipitation in the Discussion section as follows:

These results were caused by the unique characteristics of DQM. DQM overestimated the corrected extreme precipitation due to the relative variability in the data introduced through detrending, and the subsequent reintroduction of the long-term mean during the correction step widened the range of extreme precipitation, leading to overestimation compared to the reference data in areas with high variability.

1 **Intercomparison of bias correction methods for precipitation of**
2 **multiple GCMs across six continents**

3 Young Hoon Song[1], Eun-Sung Chung[1*]

4 [1] Faculty of Civil Engineering, Seoul National University of Science and Technology, 232 G
5 ongneung-ro, Nowon-gu, Seoul 01811, Korea

7 [*] Correspondence to: Eun-Sung Chung eschung@seoultech.ac.kr

9 **Abstract**

10 This study, conducted across six continents, evaluated and compared the effectiveness of three
11 Quantile Mapping (QM) methods: Quantile Delta Mapping (QDM), Empirical Quantile
12 Mapping (EQM), and Detrended Quantile Mapping (DQM) for correcting daily precipitation
13 data from 11 CMIP6 General Circulation Models (GCMs). The performance of corrected
14 precipitation data was evaluated using ten evaluation metrics, and the Technique for Order of
15 Preference by Similarity to Ideal Solution (TOPSIS) was applied to calculate performance-
16 based priorities. Bayesian Model Averaging (BMA) was used to quantify model-specific and
17 ensemble prediction uncertainties. Subsequently, this study developed a comprehensive index
18 by aggregating the performance scores from TOPSIS with the uncertainty metrics from BMA.
19 The results showed that EQM performed the best on all continents, effectively managing
20 performance and uncertainty. QDM outperformed other methods in specific regions and was
21 selected more frequently than DQM when greater weight was given to uncertainty. It suggests
22 that daily precipitation corrected by QDM is more stable than DQM. On the other hand, DQM
23 effectively reproduces dry climate but shows the highest uncertainty in certain regions,
24 suggesting potential limitations in capturing long-term climate trends. This study emphasizes
25 that both performance and uncertainty should be considered when choosing a bias correction
26 method to increase the reliability of climate predictions.

28 **Keywords**

29 CMIP6 GCM, Bias correction, Uncertainty, TOPSIS, Comprehensive index

1. Introduction

The Coupled Model Intercomparison Project (CMIP) General Circulation Models (GCMs) have provided critical scientific evidence to explore climate change (IPCC, 2021; IPCC, 2022). Nevertheless, GCMs exhibit significant biases compared to observational data for reasons such as incomplete model parameterization and inadequate understanding of key physical processes (Evin et al., 2024; Zhang et al., 2024; Nair et al., 2023). These deficiencies with GCM have introduced various uncertainties in climate projections, making ensuring sufficient reliability in climate change impact assessments difficult. In this context, many studies have proposed various bias correction methods to reduce the discrepancies between observational data and GCM simulations, thereby providing more stable results than raw GCM-based assessments (Cannon et al., 2015; Themeßl et al., 2012; Piani et al., 2010). Despite these advancements, the suggested bias correction methods differ in their physical approaches, resulting in discrepancies in the climate variables adjusted for historical periods. Furthermore, the distribution of precipitation across continents and specific locations causes variations in the correction outcomes depending on the method used, which makes it challenging to reflect extreme climate events in future projections and adds another layer of confusion to climate change research (Song et al., 2022b; Maraeun, 2013; Ehret et al., 2012; Enayati et al., 2021). Thus, exploring multiple aspects to make reasonable selections when applying bias correction methods specific to each continent and region is necessary.

Many studies have developed appropriate bias correction methods based on various theories, which have reduced the difference between GCM simulations and observed precipitation (Abdelmoaty and Papalexiou, 2023; Shanmugam et al., 2024; Rahimi et al., 2021). The Quantile Mapping (QM) series has been widely adopted among bias correction methods due to its conceptual simplicity, ease of application, and adaptability to various methodologies. However, although standard QM methods have high performance in correcting stationary precipitation, they are less efficient in non-stationary data, such as extreme precipitation events (Song et al., 2022b). To address these limitations, a recent study proposed an improved QM approach to reflect future non-stationary precipitation across all quantiles of historical precipitation (Rajulapati and Papalexiou, 2023; Cannon et al., 2015; Cannon, 2018; Song et al., 2022b). In recent years, climate studies using GCMs have adopted several improved QM methods that offer higher performance than previous methods to correct historical precipitation and project it accurately into the future. For example, Song et al. (2022b) performed bias

63 correction on daily historical precipitation over South Korea using distribution transformation

64 methods they developed and found that the best QM method varied depending on the station.

65 Additionally, previous studies have reported that QM performance varied by grid and station

66 (Ishizaki et al., 2022; Chua et al., 2022). From this perspective, these improved QMs may only

67 guarantee uniform results across some grids and regions. Therefore, to analyze positive

68 changes in future climate impact assessments, selecting appropriate bias correction methods

69 based on a robust framework is essential.

70 Multi-criteria decision analysis (MCDA) is efficient for prioritization because it can

71 aggregate diverse information from various alternatives. MCDA has been extensively used

72 across different fields to select suitable alternatives, with numerous studies confirming its

73 stability in priority selection (Chae et al., 2022; Chung and Kim, 2014; Song et al., 2024a).

74 Moreover, MCDA has been employed in future climate change studies to provide reasonable

75 solutions to emerging problems, including the selection of bias correction methods for specific

76 regions and countries (Homsi et al., 2019; Saranya and Vinish, 2021). However, MCDA's

77 effectiveness is sensitive to the source and quality of alternatives, making accurate ranking

78 challenging when information is lacking or overly focused on specific criteria (Song and Chung,

79 2016). Small-scale regional and observation-based studies have conducted GCM performance

80 evaluations, but global and continental-scale evaluations are rare due to the substantial time

81 and cost required.

82 GCM simulation includes uncertainties from various sources, such as model structure,

83 initial condition, boundary condition, and parameters (Pathak et al., 2023; Cox and Stephenson,

84 2007; Yip et al., 2011; Woldemeskel et al., 2014). The selection of bias correction methods

85 contributes significantly to uncertainty in climate change research using GCMs. Jobst et al.

86 (2018) argued that GHG emission scenarios, bias correction methods, and GCMs are primary

87 sources of uncertainty in climate change assessments across various fields. The extensive

88 uncertainties in GCMs complicate the efficient establishment of adaptation and mitigation

89 policies. This issue has increased awareness of the uncertainties inherent in historical

90 simulations. Consequently, many studies have focused on estimating uncertainties using

91 diverse methods to quantify these uncertainties (Giorgi and Mearns, 2002; Song et al., 2022a;

92 Song et al., 2023). Although it is impossible to drastically reduce the uncertainty of GCM

93 outputs due to the unpredictable nature of climate phenomena, uncertainties in GCM

94 simulations can be reduced using ensemble principles, such as multi-model ensemble

development using a rational approach (Song et al., 2024). However, accurately identifying biases in simulation precipitation remains challenging due to the lack of comprehensive equations reflecting Earth's physical processes. In this context, climate change studies have aimed to quantify the uncertainty of historical climate variables in GCMs, offering insights into the variability of GCM simulations (Pathak et al., 2023). Bias-corrected precipitation of GCMs using QM has shown high performance in the historical period, which is expected to result in better future predictions. However, the physical concepts of various QMs may lead to more significant uncertainty in the future (Lafferty et al., 2023). Therefore, efforts should be made to consider and reduce uncertainty in the GCM selection process. It will ensure the reliability of predictions by selecting an appropriate bias-correcting method.

This study aims to compare the performance of three bias correction methods using daily historical precipitation data (1980-2014) from CMIP6 GCMs across six continents (South America: SA; North America: NA; Africa: AF; Europe: EU; Asia: AS; and Oceania: OA). Ten evaluation metrics were used to assess the performance of daily precipitation corrected by the three QM methods for each continent. Subsequently, the Technique for Order of Preference by Similarity to Ideal Solution (TOPSIS) of MCDA was applied to select an appropriate bias correction method for each continent. Additionally, the uncertainty in daily precipitation for historical periods was quantified using Bayesian Model Averaging (BMA). By integrating performance scores from TOPSIS and uncertainty metrics from BMA, this study developed a Comprehensive Index (CI), which was then used to select the best bias correction method for each continent. This comprehensive approach ensures a balanced consideration of both performance and uncertainty, enhancing understanding of the bias correction process based on the distribution of daily precipitation across continents.

2. Datasets and methods

2.1 General Circulation Model

This study used 11 CMIP6 GCM to perform bias correction for daily precipitation in the historical period. This study used daily precipitation to correct bias because the natural variability relative to projected anthropogenically forced trends is much larger for precipitation than for temperature (Deser et al., 2012). Table 1 presents basic information, including model names, resolution, and variant labels. The model resolution of 11 CMIP6 GCMs was equally

126   re-gridded to 1°×1° using linear interpolation. Furthermore, this study's ensemble member of

127   CMIP6 GCMs was the first member of realizations (r1).

128

129   Table 1. Information of CMIP6 GCMs in this study

Models	Resolution	Climate variables	Variant label
ACCESS-CM2	1.2° × 1.8°	Daily precipitation	r1i1p1f1
ACCESS-ESM1-5	1.2° × 1.8°		
BCC-CSM2-MR	1.1° × 1.1°		
CanESM5	2.8° × 2.8°		
CESM2-WACCM	0.9° × 1.3°		
CMCC-CM2-SR5	~ 0.9°		
CMCC-ESM2	0.9° × 1.25°		
EC-Earth3-Veg-LR	1.0° × 1.0°		
GFDL-ESM4	1.4° × 1.4°		
INM-CM4-8	~ 0.9°		
IPSL-CM6A-LR	1.1° × 1.1°		

130

131   **2.2 Reference data**

132   This study utilized ERA5 reanalysis data from the European Center for Medium-Range

133   Weather Forecasts (ECMWF) as reference data. The model physics of ERA5 reanalysis data

134   improved as it employed an Integrated Forecasting System based on CY41r2 (Hersbach et al.,

135   2020). ERA5 has been widely used in various studies to ensure the reliability of climate model

136   evaluation and climate change assessment (Jeong et al., 2024; Virgilio et al., 2024; Baek et al.,

137   2024). The model resolution selected in this study was 1.0° × 1.0°, which was provided by the

138   institution for research availability. The accuracy of assessing GCM simulation is crucial for

139   replicating the spatial and temporal variability of observed data (Hamed et al., 2023). In this

140   context, the ERA5 product has been commonly used to reproduce observed precipitation, for

141   the evaluation of GCMs' performances.

142

143   **2.3 Quantile mapping**

144   This study employed three (Quantile delta mapping, QDM; Detrended quantile mapping, DQM;

145   Empirical quantile mapping, EQM) QM methods to correct the simulation of CMIP6 GCMs,

146   and these methods are commonly used in climate change research based on the climate models

147   (Switanek et al., 2017). This study divided the data into a training period (1980-1996) and a

148   validation period (1997-2014) to correct the historical period's data. This approach minimizes

149   the influence of uncertainties associated with future projections, allowing the study to focus on

150 evaluating the intrinsic performance differences of the QM methods. The frequency-adaptation

151 technique, as described by Themeßl et al. (2012), was applied to address potential biases and

152 improve the accuracy of the corrections. The corrected precipitation using the QM used a

153 cumulative distribution function, as shown in Equation 1, to reduce the difference from the

154 reference data.

155 $\hat{x}_{m,p}(t) = F_{o,h}^{-1}\{F_{m,h}[x_{m,p}(t)]\}$ (1)

156 where, $\hat{x}_{m,p}(t)$ presents the bias-corrected results. $F_{o,h}$ represents the cumulative distribution

157 function (CDF) of the observed data, and $F_{m,h}$ presents the CDF of the model data. The

158 subscripts o and m denote observed and model data, respectively, and the subscript h denotes

159 the historical period.

160 QDM, developed by Cannon et al. (2015), preserves the relative changes ratio of modeled

161 precipitation quantiles. In this context, QDM consists of bias correction terms derived from

162 observed data and relative change terms obtained from the model. The computation process of

163 QDM is carried out as described in Equation (2) to (4).

164 $\hat{x}_{m,p}(t) = \hat{x}_{o:m,h:p}(t) \cdot \Delta_m(t)$ (2)

165 $\hat{x}_{o:m,h:p}(t) = F_{o,h}^{-1}[F_{m,p}^{(t)}\{x_{m,p}(t)\}]$ (3)

166 $\Delta_m(t) = \dfrac{x_{m,p}(t)}{F_{m,h}^{-1}[F_{m,p}^{(t)}\{x_{m,p}(t)\}]}$ (4)

167 where, $\hat{x}_{o:m,h:p}(t)$ presents the bias corrected daily precipitation for the historical period, and

168 $\Delta_m(t)$ the relative change in the model simulation between the reference period and the target

169 period. In addition, the target period is calculated by multiplying the relative change ($\Delta_m(t)$)

170 at time (t) multiplied by the bias-corrected precipitation in the reference period. $\Delta_m(t)$ is

171 defined as $\widehat{x_{m,p}}(t)$ divided by $F_{o,h}^{-1}[F_{m,p}^{(t)}\{x_{m,p}(t)\}]$. $\Delta_m(t)$ preserving the relative change

172 between the reference and target periods. DQM, while more limited compared to QDM,

173 integrates additional information regarding the projection of future precipitation. Furthermore,

174 climate change signals estimated from DQM tend to be consistent with signals from baseline

175 climate models. The computational process of DQM is performed as shown in Equation (5).

176 $\hat{x}_{m,p} = F_{o,h}^{-1}\left\{F_{m,h}\left[\dfrac{\bar{X}_{m,h}X_{m,h}(t)}{\bar{X}_{m,p}(t)}\right]\right\}\dfrac{\bar{X}_{m,p}(t)}{\bar{X}_{m,h}}$ (5)

177 where, $\bar{X}_{m,h}$ and $\bar{X}_{m,p}$ represent the long-term modeled averages for the historical reference

178 period and the target period, respectively.

179 EQM is a method that corrects the quantiles of the empirical cumulative distribution function

180 from a GCM simulation based on a reference precipitation distribution using a corrected

181 transfer function (Dequé, 2007). The calculation process of EQM can be represented as follows

182 in Equation (6).

183 $\hat{x}_{m,p}(t) = F_{o,h}^{-1}(F_{m,h}(x_{m,p}(t)))$ (6)

184 All these QMs can be applied to historical data correction in this approach. The bias correction

185 is performed based on the relative changes between a reference period and a target period in

186 the past, ensuring that the relative changes between these periods are preserved in the corrected

187 data (Ansari et al., 2023; Tanimu et al., 2024; Cannon et al., 2015).

188

189 **2.4 Evaluation metrics**

190 This study used ten evaluation metrics to assess the output performance of three quantile

191 mapping methods against the reference data for the validation period (1997-2014). Seven

192 evaluation metrics used in this study are as follows: Root Mean Square Error (RMSE), Mean

193 Absolute Error (MAE), Coefficient of Determination (R^2), Percent bias (Pbias), Nash-Sutcliffe

194 Efficiency (NSE), Kling-Gupta efficiency (KGE), Median Absolute Error (MdAE), Mean

195 Squared Logarithmic Error (MSLE), Explained Variance Score (EVS), and Jenson-Shannon

196 divergence (JS-D). The equations of seven evaluation metrics are presented in Table 2.

197

198 Table 2. Information of the seven-evaluation metrics used in this study

Metrics	Equations	Factors	References
RMSE	$= \sqrt{\dfrac{1}{n}\sum_{i=1}^{n}\left(X_i^{sim} - X_i^{ref}\right)^2}$	X_i^{ref} reference data X_i^{sim} Bias corrected GCM	
MAE	$= \sum_{i=1}^{n}\left|X_i^{sim} - X_i^{ref}\right|$		
R^2	$= 1 - \dfrac{\sum_{i=1}^{n}(X_i^{sim} - X_i^{ref})^2}{(X_i^{ref} - \bar{X}_i^{ref})^2}$		Galton, 1886
Pbias	$= \dfrac{\sum_{i=1}^{n}(X_i^{ref} - X_i^{sim})}{\sum_{i=1}^{n} X_i^{ref}} \times 100$		

NSE	$$= 1 - \frac{\sum_{i=1}^{n}(X_i^{sim} - X_i^{ref})^2}{\sum_{i=1}^{n}(X_i^{ref} - \bar{X}_i^{ref})^2}$$		Nash and Sutcliffe, 1970
MdAE	$$= median(|X_i^{sim} - X_i^{ref}|)$$		
MSLE	$$= \frac{1}{n}\sum_{i=1}^{n}(\log(1 + X_i^{sim}) - \log(1 + X_i^{ref}))^2$$		
EVS	$$= 1 - \frac{Var(X^{sim} - X^{ref})}{Var(X^{ref})}$$		
KGE	$$= 1 - \sqrt{(r-1)^2 + (\alpha - 1)^2 + (\beta - 1)^2}$$	r Pearson product-moment correlation α Variability error β: Bias term	Gupta et al. 2009
JS-D	$$= \frac{1}{2}D_{KL}\left(P \parallel \frac{P+Q}{2}\right) + \frac{1}{2}D_{KL}\left(Q \parallel \frac{P+Q}{2}\right)$$	$P(x)$: Probability density distribution of reference data $Q(x)$: Probability density distribution of GCM D_{KL}: KL-D	Lin, 1991

Ten evaluation metrics selected in this study assess GCM performance from various perspectives, including error (RMSE, MAE, MdAE, and MSLE), deviation (Pbias), accuracy (R^2, NSE), variability (EVS), correlation and overall performance (KGE), and distributional differences (JSD). These metrics complement each other by offering a comprehensive evaluation framework. For instance, while NSE evaluates the overall fit of the simulated data to observations, KGE provides a holistic view by integrating correlation, variability, and bias into a single efficiency score, and JS-D captures the difference between the distributions of the reference data and the bias-corrected GCM output.

2.5 Generalized extreme value

210   This study used generalized extreme value (GEV) to compare the extreme precipitation
211   calculated by the bias-corrected GCM at each grid of six continents over the historical period.
212   The historical precipitation was compared with the distribution of reference data and bias-
213   corrected GCM above the 95th quantile of the Probability Density Function (PDF) of the GEV
214   distribution (Hosking et al. 1985). In addition, this study compared the distribution differences
215   between the reference data based on the GEV distribution and the corrected GCM using JSD.
216   GEV distribution is commonly used to confirm extreme values in climate variables. The PDF
217   of the GEV distribution is shown in Equation 7, and the parameters of the GEV distribution
218   were estimated using L-moment (Hosking, 1990).

219   $$g(x) = \frac{1}{\alpha} \left[1 - k \frac{x-\epsilon}{\alpha} \right]^{\frac{1}{k}-1} exp \left\{ - \left[1 - k \frac{x-\epsilon}{\alpha} \right]^{\frac{1}{k}} \right\} \quad (7)$$

220   where, k, α, and ε represents a shape, scale, and location of the GEV distribution, respectively.
221

222   2.6 Bayesian model averaging (BMA)

223   The BMA is a statistical technique that combines multiple models to provide predictions that
224   account for model uncertainty (Hoeting et al., 1999). BMA is used to integrate predictions from
225   GCMs to improve the robustness and reliability of the resulting assemblies. The posterior
226   probability of each model is calculated based on Bayes' theorem as shown in Equation 8.

227   $$P(M_k \mid D) = \frac{P(D|M_k)P(M_k)}{\sum_{j=1}^{K} P(D|M_j)P(M_j)} \quad (8)$$

228   where, $P(M_k)$ is the prior probability of model M_k, and $P(D \mid M_k)$ s the likelihood of the data
229   D given model M_k, $P(M_k \mid D)$ is the posterior probability of model M_k. In addition, the BMA
230   prediction $\hat{Q}_{BMA}$ is the weighted average of the predictions from each model as shown in
231   Equation 9.

232   $$\hat{Q}_{BMA} = \sum_{k=1}^{K} P(M_k \mid D)\hat{Q}_k \quad (9)$$

233   where, $\hat{Q}_k$ is the prediction from model M_k. In this study, BMA was used to quantify the model
234   uncertainty and ensemble prediction uncertainty for daily precipitation corrected by three QM
235   methods (QDM, EQM, and DQM) applied to 11 CMIP6 GCMs, as shown in Equations 10 and
236   11.

237   $$\alpha_w^2 = \frac{1}{K} \sum_{k=1}^{K} (w_k - \overline{w})^2 \quad (10)$$

238 where, K is the number of models, $w_k = P(M_k \mid D)$ is the weight of model M_k, $\overline{w}$ is the mean

239 of the weights, given by $\overline{w} = \frac{1}{K}\sum_{k=1}^{K} w_k$. A higher variance in model weights indicates more

240 significant prediction differences, implying greater model uncertainty.

241 $\sigma BMA = \sqrt{\frac{1}{K}\sum_{k=1}^{K}(\hat{Q}_k - \hat{Q}BMA)^2}$ (11)

242 σBMA is standard deviation of the BMA ensemble predictions, $\hat{Q}_k$ is the prediction from each

243 model M_k, $\hat{Q}BMA$ is the weighted average prediction from BMA. This standard deviation

244 represents the variability among the ensemble predictions and serves as an indicator of

245 uncertainty. A lower standard deviation implies higher consistency among predictions,

246 indicating lower uncertainty, while a higher standard deviation suggests greater variability and

247 higher uncertainty.

248

249 **2.7 TOPSIS**

250 This study used TOPSIS to calculate a rational priority among three QM methods based on the

251 outcomes derived from evaluation metrics. Furthermore, the closeness coefficient calculated

252 using TOPSIS was used as the performance metric for the CI. Proposed by Hwang and Yoon

253 (1981), TOPSIS is a multi-criteria decision-making technique frequently used in water

254 resources and climate change research to select alternatives (Song et al., 2024). As described

255 in Equation 12 and 13, the proximity of the three QM methods is calculated based on the

256 Positive Ideal Solution (PIS) and the Negative Ideal Solution (NIS).

257 $D_i^+ = \sqrt{\sum_{j=1}^{n} w_j(f_j^+ - f_{i,j})^2}$ (12)

258 $D_i^- = \sqrt{\sum_{j=1}^{n} w_j(f_j^- - f_{i,j})^2}$ (13)

259 where, D_i^+ is the Euclidean distance of each criterion from the PIS, summing the whole criteria

260 for an alternative f_j^+, j presents the normalized value for the alternative f_j^+. w_j presents weight

261 assigned to the criterion j. D_i^- is the distance between the alternative f_j^- and the NIS. The

262 relative closeness is calculated as shown in Equation 14. The optimal value is closer to 1 and

263 represents a reasonable alternative.

264 $C_i = \frac{D_i^-}{(D_i^- + D_i^+)}$ (14)

2.8 Comprehensive index (CI)

This study proposed a CI to select the best QM method by combining performance scores and model uncertainty indicators. The CI integrates the performance scores (closeness coefficient) derived from the TOPSIS method with the uncertainty quantified using BMA. This approach allows for a balanced evaluation that considers both the effectiveness of the QM methods and the associated uncertainties. Uncertainty was quantified in two ways. Model-specific weight variance was calculated using the variance of the model weights assigned by BMA, representing the uncertainty in selecting the appropriate QM. The standard deviation of BMA ensemble prediction was calculated to capture the spread and, thus, the uncertainty of the ensemble forecasts. Both the indicators were normalized using a min-max scaler to ensure comparability. The CI is calculated individually for every grid and can reflect climate characteristics. Framework provides flexibility in determining the weighting of uncertainty or performance depending on the study objectives. Additionally, the methodology offers flexibility in selecting performance and uncertainty metrics. Alternative MCDA methods beyond TOPSIS can be utilized for performance indicators, or indices that effectively represent the model's performance can be employed to calculate the CI. Similarly, for uncertainty indicators, approaches such as variance, standard deviation, or other uncertainty quantification techniques can be applied to enhance the robustness of the framework further. Finally, the calculation process of the CI is performed as shown in Equations 15 and 16.

$$UI = \frac{V_w + \sigma_e}{2} \quad (15)$$

$$CI = \alpha \times C_i - \beta \times UI \quad (16)$$

where, UI represents the uncertainty indicator. V_w and σ_e represent the normalized weight variance and the normalized ensemble standard deviation, respectively, calculated using BMA. C_i represents the closeness coefficient calculated from TOPSIS. α represents the weight given to the performance score, β represents the weight given to the uncertainty indicator. Furthermore, by adjusting the weights α and β, the study evaluated the QM methods under different scenarios. Equal weight ($\alpha = 0.5$, $\beta = 0.5$) balances performance and uncertainty equally, and the emphasized performance weight ($\alpha = 0.7$, $\beta = 0.3$) prioritize performance over

297 uncertainty. The emphasized uncertainty weight ($\alpha= 0.3$, $\beta=0.7$) prioritize uncertainty over

298 performance. The results from the CI provide a holistic evaluation of the QM methods,

299 considering both their effectiveness in bias correction and the reliability of their predictions.

300

301 **3. Result**

302 **3.1 Assessment of bias correction reproducibility across continents**

303 **3.1.1 Comparison of bias correction effects**

304 This study applied three QM methods to correct daily precipitation data from 11 CMIP6 GCMs

305 across six continents. Figure 1 presents the results of comparing daily precipitation data before

306 and after bias correction using the Taylor diagram. In general, the precipitation corrected by

307 DQM showed a larger difference from the reference data than other methods. In contrast, EQM

308 performed better than DQM, and many models showed results close to the reference data. The

309 precipitation corrected by QDM also showed good performance in most continents but slightly

310 lower than EQM. Nevertheless, QDM showed clearly better results than DQM.

311 Regarding correlation coefficients, precipitation corrected by DQM showed relatively high

312 values between 0.8 and 0.9 but lower than EQM and QDM. The precipitation corrected by

313 EQM showed high agreement with the reference data, recording correlation coefficients above

314 0.9 in most continents. QDM generally showed similar correlation coefficients to EQM but

315 slightly lower values than EQM in North America and Asia.

316 For RMSE, precipitation corrected by DQM was higher than EQM and QDM, indicating that

317 the corrected precipitation differed more from the reference data. On the other hand, EQM had

318 the lowest RMSE and showed superior performance compared to other methods. QDM had

319 slightly higher RMSE than EQM but still outperformed DQM.

320 In terms of standard deviation, precipitation corrected by DQM was higher or lower than the

321 reference data in most continents. On the other hand, precipitation corrected by EQM was

322 similar to the reference data and almost identical to the reference data in Africa and Asia. QDM

323 was similar to the reference data in some continents but showed slight differences from EQM.

324 These results imply that the precipitation corrected by the three methods outperforms the raw

325 simulation, which confirms that the GCM's daily precipitation is reliably corrected in the

326 historical period.

327

Taylor diagram

(a) South America
(b) North America
(c) Africa
(d) Europe
(e) Asia
(f) Oceania
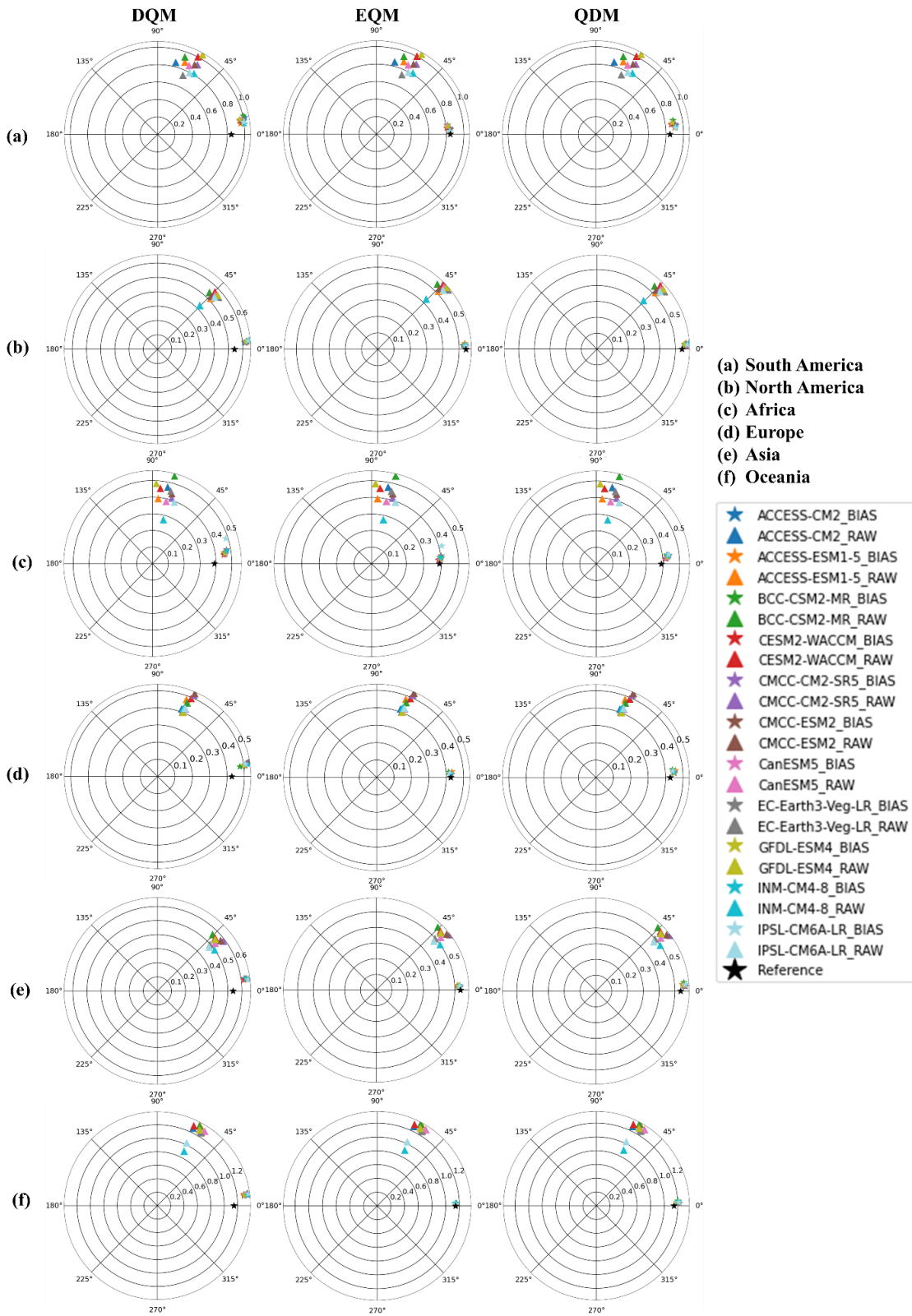
328

329   Figure 1. Comparison of raw and corrected daily precipitation on six continents using Taylor

330   diagrams

3.1.2 Spatial distribution of bias correction performance

331

332 This study evaluated the performance of daily precipitation across six continents using ten

333 evaluation metrics for 11 CMIP6 GCMs. Figures 2 and S1 present the spatial patterns of these

334 evaluation metrics, calculated for daily precipitation from the bias corrected GCMs in South

335 America. Overall, the precipitation corrected by EQM demonstrated lower JSD values, as well

336 as higher EVS and KGE values, compared to other methods. The precipitation corrected by

337 EQM showed higher EVS in certain regions but slightly lower performance in MdAE and Pbias

338 across some grids. DQM exhibited performance similar to EQM and QDM in most evaluation

339 indices but was relatively lower in most evaluation metrics. The precipitation corrected by the

340 three methods was underestimated compared to the reference data in northern South America,

341 while it was overestimated in eastern South America. In addition, precipitation corrected by

342 the DQM method tended to be overestimated more than the other methods, while the EQM

343 method showed the opposite result. Furthermore, the daily precipitation corrected by EQM

344 showed the lowest overall error and high performance in both NSE and R^2. QDM and DQM

345 also performed well but exhibited slightly larger errors in some regions than EQM.

346
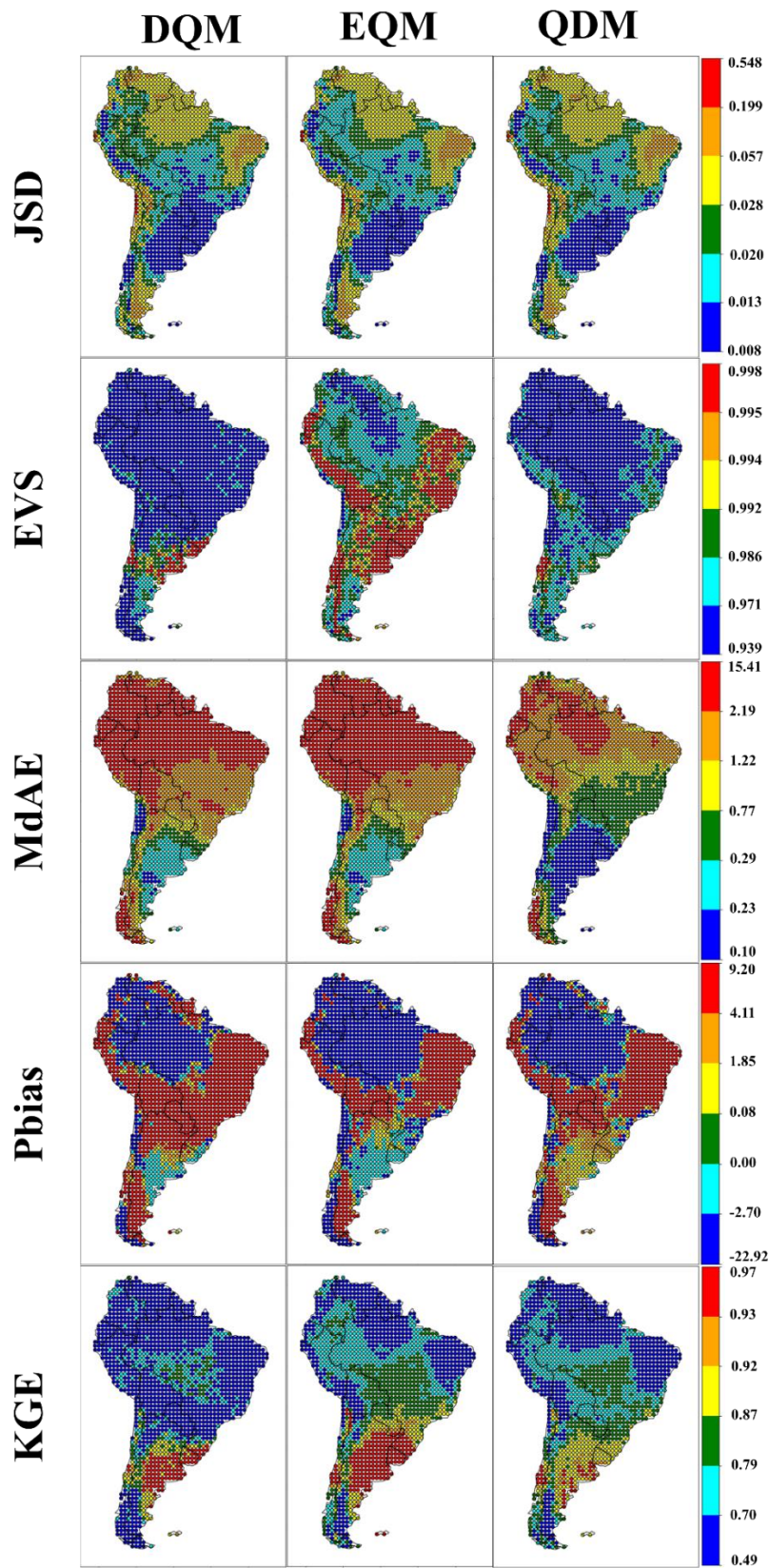
347

348 Figure 2. Performance comparison of DQM, EQM, and QDM using evaluation metrics (JSD,

349 EVS, MdAE, Pbias, and KGE) for daily precipitation in South America.

350   Figures 3 and S2 present the spatial patterns of these evaluation metrics, calculated for daily

351   precipitation from the bias corrected GCMs in South America. Regarding error metrics (MAE,

352   MSLE, RMSE, and MdAE), precipitation corrected using DQM showed relatively lower

353   performance across North America, with substantial errors in the southern region. In contrast,

354   precipitation corrected using EQM demonstrated superior performance across the continent

355   compared to other methods. QDM exhibited similar error performance to EQM but slightly

356   higher errors in the southern region.

357   For correlation metrics (NSE and R^2), DQM-corrected precipitation had lower performance

358   than other methods, although some grid cells in the central and eastern regions showed high

359   performance, with values exceeding 0.995. The precipitation corrected using EQM showed the

360   highest performance, especially in the central and eastern regions, where most grid points

361   showed correlation coefficients above 0.995. QDM, while achieving correlation metrics above

362   0.978 for most grid points, had slightly lower performance than the other methods.

363   Regarding Pbias, all three methods tended to overestimate precipitation relative to the reference

364   data across most grid points in North America, while corrected precipitation in Greenland was

365   underestimated. For JSD, EVS, and KGE metrics, EQM-corrected precipitation showed the

366   highest performance, with DQM and QDM performing lower than EQM.

367
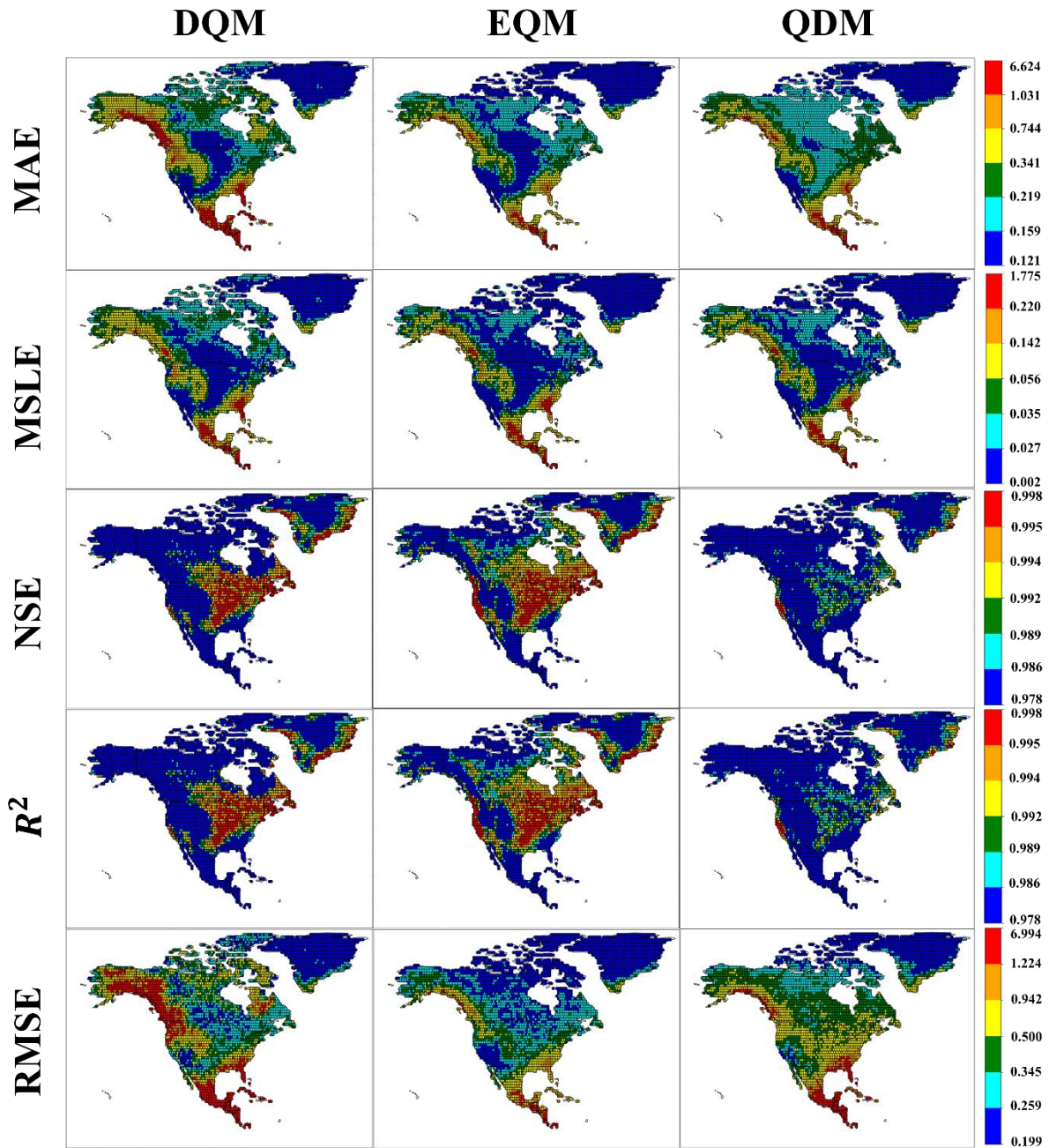
368

369 Figure 3. Performance comparison of DQM, EQM, and QDM using evaluation metrics (MAE,

370 MSLE, NSE, R^2, and RMSE) for daily precipitation in North America.

371

372 In this study, the daily precipitation in Africa was corrected using three QM methods, and the

373 performance is shown in Figures 4 and S3. Overall, the JSD of precipitation corrected by the

374 three methods showed similar spatial patterns, but the precipitation of DQM showed lower

375 performance than the other methods in the southern region. In terms of EVS, the precipitation

376 of DQM showed higher variability than the other methods. The precipitation of QDM showed

377 lower variability in southern Africa than DQM, but overall, it showed higher variability than

378 EQM. The precipitation of EQM showed lower variability in southern and central Africa but

379 still showed high variability in the northern region. Analyzing the error performance, the

380 precipitation corrected by QDM showed the best performance compared to the other methods.

381 In particular, QDM showed the highest performance in North Africa (MAE: 0.03, and MSLE:

382 0.004), and EQM's error performance was lower than QDM's in most indicators but better than

383 DQM's. Finally, EQM performed the highest in correlation metrics (NSE and R^2), and QDM

384 performed better than DQM.
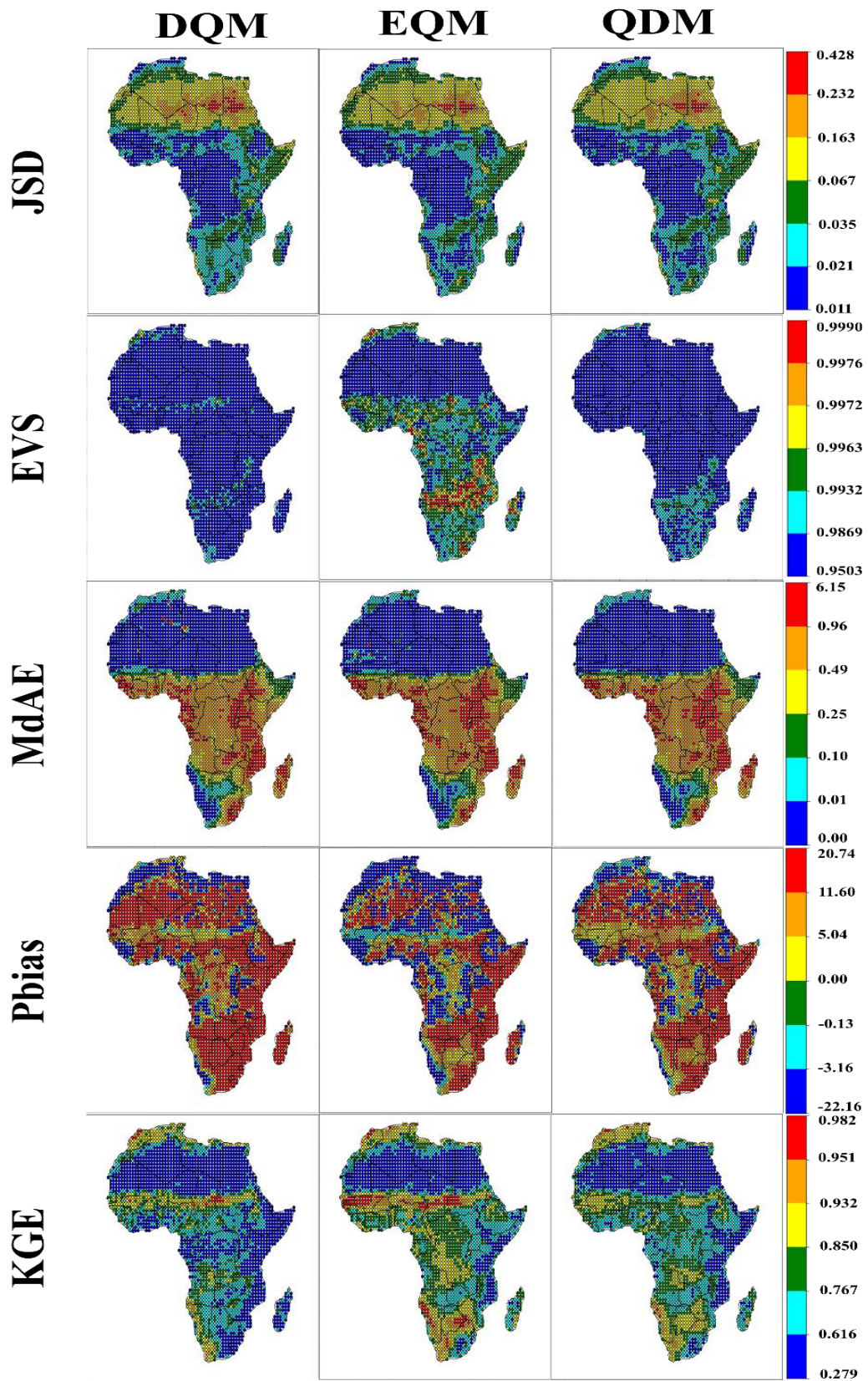
385

386 Figure 4. Performances of DQM, EQM, and QDM using evaluation metrics (JSD, EVS, MdAE,

387 Pbias, and KGE) for daily precipitation in Africa.

388   Figures 5 and S4 show the spatial results of the grid-based evaluation metrics for the European

389   region. In terms of error metrics, EQM-corrected precipitation performed the best across

390   Europe compared to other methods. In contrast, QDM-corrected precipitation performed

391   similarly to DQM in MAE and MSLE but significantly outperformed DQM in RMSE.

392   Regarding NSE and R, EVS, and KGE metrics, EQM-corrected precipitation performed

393   overwhelmingly better than other methods. QDM precipitation performed better than DQM,

394   while DQM performed the worst. Regarding Pbias, EQM-corrected precipitation was

395   underestimated compared to the reference data in most parts of Europe. In contrast, QDM-

396   corrected precipitation was more similar to the reference data compared to other methods, and

397   DQM precipitation was overestimated compared to the reference data except in central Europe.

398
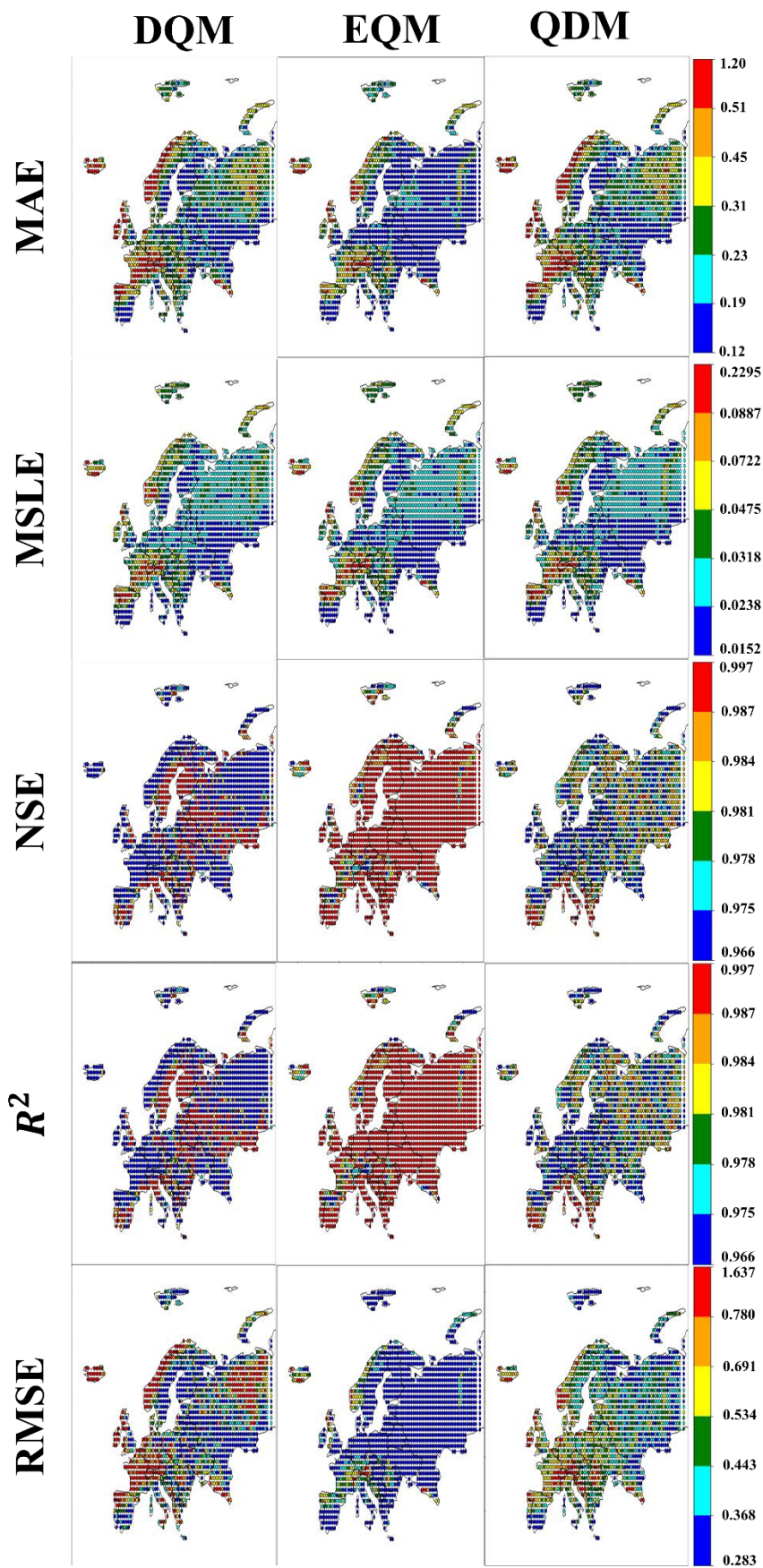
399   Figure 5. Performances of DQM, EQM, and QDM using evaluation metrics (MAE, MSLE,

400   NSE, R^2, and RMSE) for daily precipitation in Europe.

401   Figures 6 and S5 show the results of spatially quantifying the corrected precipitation in Asia

402   using various evaluation metrics. Regarding error metrics, EQM-corrected precipitation stands

403   out with its superior performance, particularly in RMSE, which was consistently below 1.35 in

404   most areas except for certain parts of Central Asia. In contrast, DQM-corrected precipitation

405   showed the poorest performance in error metrics. QDM-corrected precipitation demonstrated

406   a performance similar to EQM but slightly lower in East Asia and North Asia. In NSE and R,

407   the precipitation corrected by EQM performed better than other methods, especially in

408   Southwest and East Asia. In contrast, the precipitation corrected by DQM performed lower

409   than other methods. Regarding EVS, the precipitation corrected by EQM showed the lowest

410   variability, while QDM showed higher variability than EQM but lower variability than DQM.

411   In the case of Pbias, precipitation corrected by DQM was overestimated compared to the

412   reference data throughout Asia. The precipitation corrected by EQM was underestimated in

413   most regions except Central Asia. Precipitation in QDM showed a similar spatial pattern to that

414   in EQM, but the range of Pbias was more diverse.

415

416
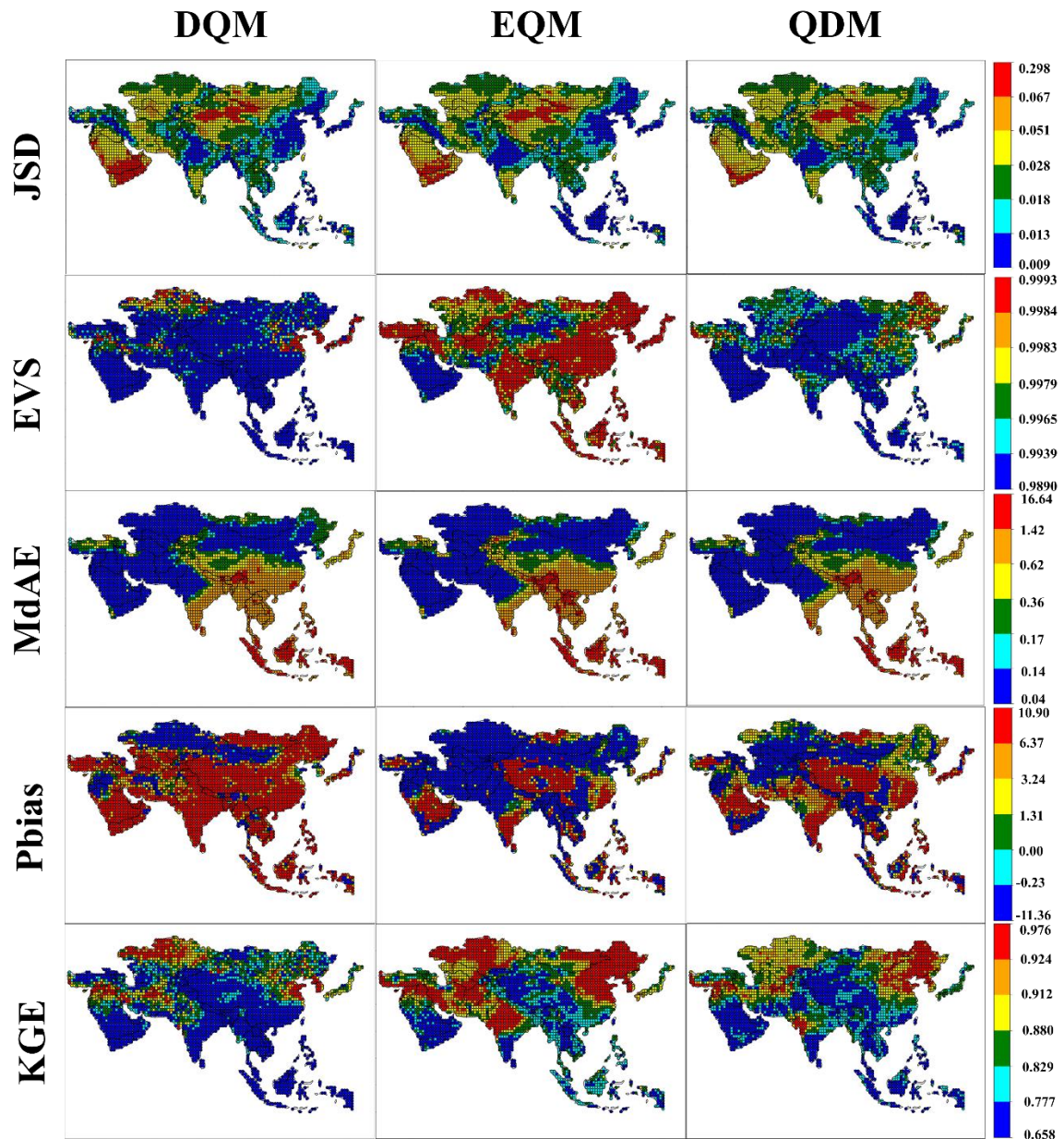
Figure 6. Performances of DQM, EQM, and QDM using evaluation metrics (JSD, EVS, MdAE,

Pbias, and KGE) for daily precipitation in Asia.

419

Figures 7 and S6 show the results of spatially quantifying the corrected daily precipitation in

Oceania using various evaluation metrics. In terms of error metrics, the precipitation estimated

by the three QM methods performed similarly in MAE, MdAE, and MSLE. However, the

precipitation corrected by EQM performed better in RMSE than the other methods. In the case

of JSD, all three methods performed well.

425 Regarding EVS, the precipitation corrected by EQM showed lower variability than the other
426 methods, and DQM showed higher performance than QDM. In Pbias, the precipitation adjusted
427 by QDM was overestimated compared to the reference data in Oceania, while the precipitation
428 corrected by DQM and EQM was underestimated compared to the reference data in central and
429 southern Oceania. Finally, in KGE, precipitation corrected by EQM showed the highest
430 performance, while DQM showed the lowest.

431
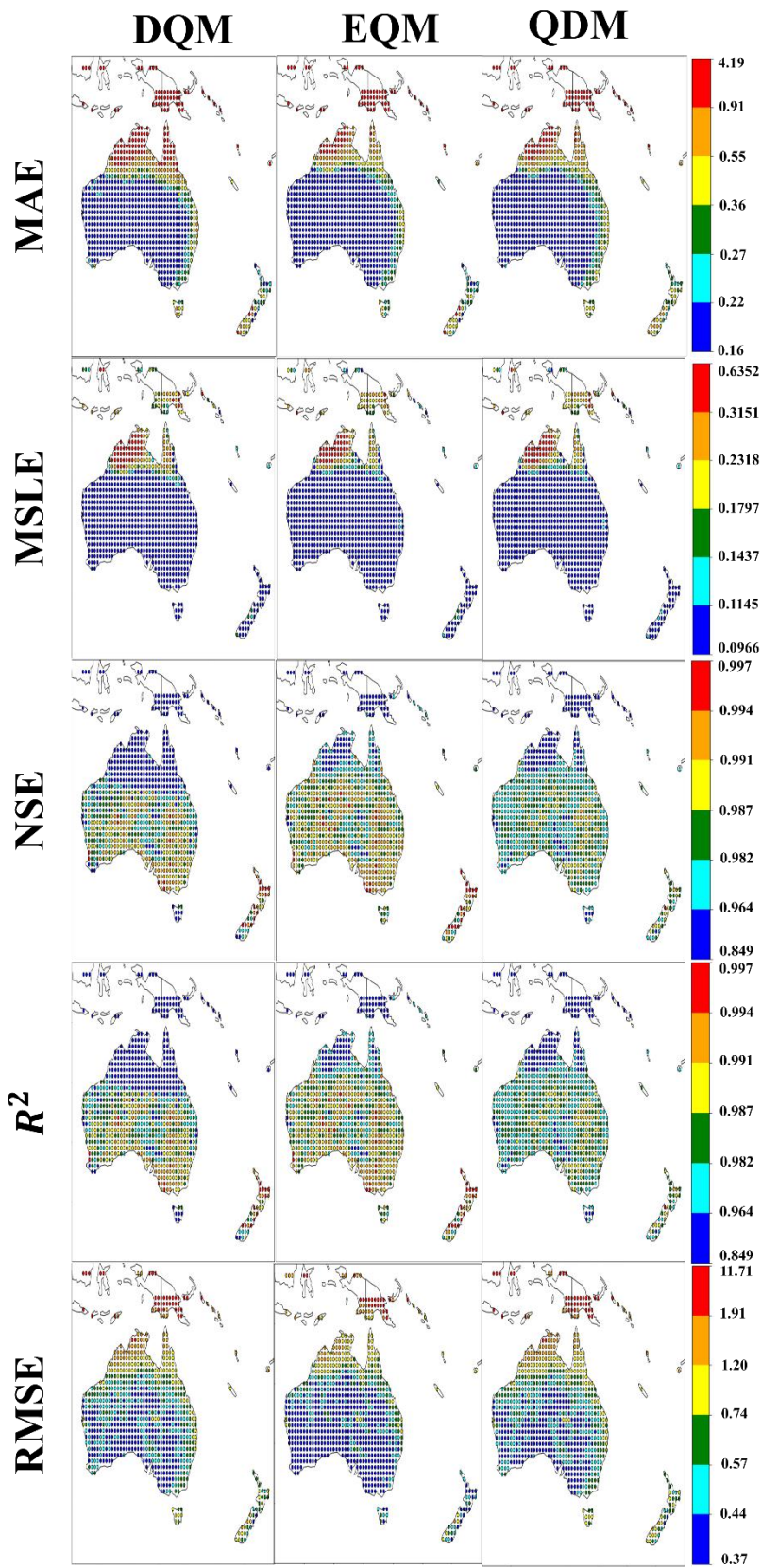
Figure 7. Performances of DQM, EQM, and QDM using evaluation metrics (MAE, MSLE,

433   NSE, R^2, and RMSE) for daily precipitation in Asia.

434   Figure 8 visualizes the results of evaluating the bias-corrected precipitation data using 11

435   CMIP6 GCMs on six continents using ten evaluation metrics as boxplots. Overall, the

436   precipitation corrected by EQM outperforms the other methods on most continents. In

437   particular, EQM performs the best on the error metrics. QDM performs slightly lower than

438   EQM but still maintains a high level of performance on all continents. On the other hand, DQM

439   has more significant errors and relatively poor performance compared to the other methods on

440   most metrics.

442 Figure 8. Performances of DQM, EQM, and QDM of historical period precipitation using

443 boxplots based on ten evaluation metrics

3.1.3 Comparison of reproducibility for extreme daily precipitation

This study compared the daily extreme precipitation corrected by three methods using the GEV distribution. Figure 9 compares the distribution differences of the daily precipitation adjusted by the biased bias correction methods based on the GEV distribution using the JSD. In general, the JSD values for precipitation from DQM, EQM, and QDM are very low for most continents, indicating that the GEV distributions are almost identical among the three methods. Although there are some outliers, the overall distribution differences are not significant, suggesting little difference among the three methods when correcting for historical precipitation. However, in Europe, unlike other continents, the differences between the first and third quartiles of the JSD are relatively significant, indicating that the distributions can vary significantly from grid to grid depending on the QM method.
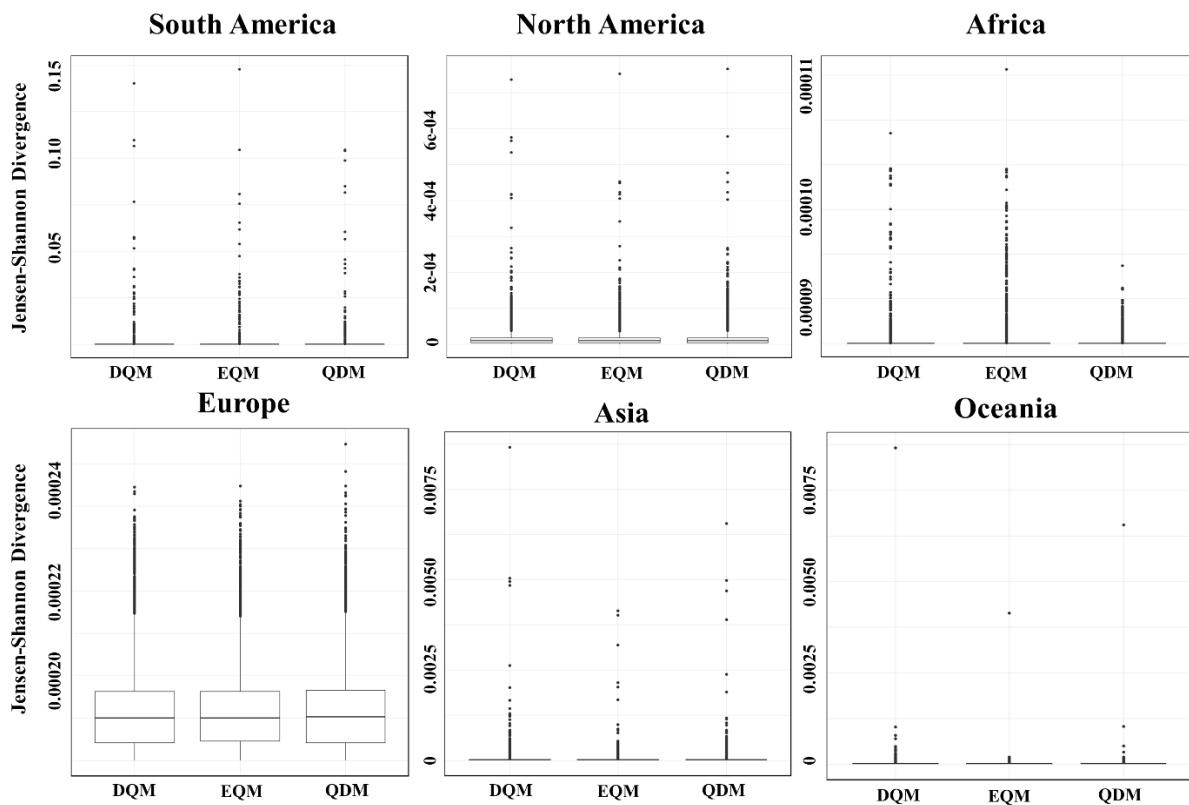
Figure 9. Comparison of distribution differences for GEV distribution using JSD across six continents.

Figure 10 shows the probability density functions for extreme precipitation above the 95th percentile of the GEV distribution. Overall, DQM shows the highest probability density for

extreme precipitation across all continents and has the widest distribution, indicating that DQM corrects more extreme precipitation. On the other hand, EQM shows the lowest probability density and conservatively corrects for extreme precipitation. QDM shows probability densities between EQM and DQM across most continents but closer to EQM.
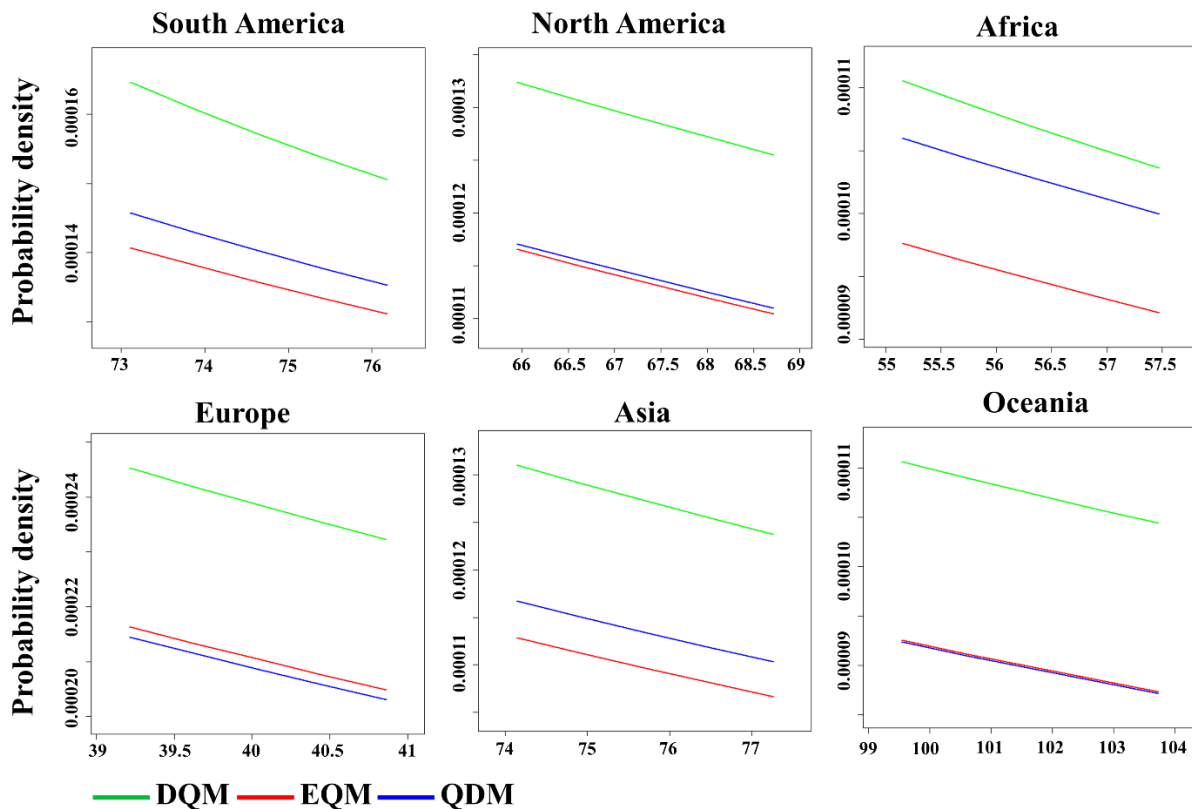
Figure 10. Comparison of probability densities for extreme precipitation values above the 95th percentile using GEV.

3.2 Prioritization of bias correction methods based on performance

3.2.1 Results of weight for evaluation metrics

In this study, the weights were calculated by applying entropy theory to the evaluation metrics used in the TOPSIS analysis, and the results are presented in Table 3. JSD had the highest weight in South America because the estimated JSD from 11 CMIP6 GCMs was an important metric for evaluating model performance differences. These results indicate that the differences between distributions are significant. On the other hand, EVS and NSE in South America had very low weights, suggesting that the variability and efficiency of precipitation were considered less important than other indicators. For North America, the RMSE, MSLE, and MAE metrics were of significant importance, as evidenced by their high weights. These error metrics

481   revealed substantial regional differences. In contrast, EVS carried a negligible weight,
482   suggesting it was less important in explaining variability in North America. For Africa, MdAE
483   and JSD metrics were of considerable importance, as indicated by their high weights. These
484   metrics were key evaluation factors in Africa. Conversely, EVS carried a low weight,
485   suggesting it was considered relatively less important. RMSE had the highest weight in Europe,
486   and KGE also had a relatively high weight, indicating that these metrics were considered
487   important evaluation criteria in Europe. In Asia, MAE and MSLE had high weights, suggesting
488   that these metrics were important evaluation metrics. On the other hand, EVS and NSE were
489   considered less important due to their low variability. JSD, KGE, RMSE, and MAE were
490   assigned high weights in Oceania, indicating that these metrics are essential factors. On the
491   other hand, R^2 and NSE were assigned low weights.

492

493   Table 3. Entropy-based weights for evaluation metrics across different continents

	RMSE	MAE	R^2	NSE	KGE	Pbias	MdAE	MSLE	EVS	JSD
South America	0.1439	0.1536	0.0001	0.0001	0.0005	0.0238	0.1754	0.1934	0.0004	0.3088
North America	0.2289	0.1908	0.0001	0.0001	0.0007	0.0118	0.2152	0.2117	0.0001	0.1411
Africa	0.1319	0.1686	0.0002	0.0002	0.0002	0.0855	0.2436	0.1911	0.0002	0.1786
Europe	0.2821	0.1762	0.0022	0.0022	0.0063	0.0378	0.1754	0.1666	0.0021	0.1490
Asia	0.2073	0.1954	0.00003	0.00003	0.0001	0.0305	0.2300	0.2024	0.00003	0.1342
Oceania	0.2384	0.2204	0.0013	0.0013	0.0068	0.0214	0.2338	0.2093	0.0012	0.0660

494

495   **3.2.2 Selection of the best bias correction method based on TOPSIS**
496   Figures 11 and S7 present the best bias correction method selected for each continent using the
497   TOPSIS approach. In Figure 11(a), the spatial distribution of the most effective bias correction
498   method across the grid points of each continent is shown. In contrast, Figure 11(b) shows the
499   number of grid points selected for each QM method. In South America, EQM was chosen as
500   the best method in most grid points, with EQM being selected in over 1,500 grid points. In
501   contrast, QDM was selected in fewer than 700 grid cells, making it the least chosen method in
502   South America. Across all continents except South America, EQM was selected as the best
503   model in the majority of grid cells, with the number of selected grid points (North America:
504   7,583; Africa: 2,879; Europe: 2,719; Asia: 8,793; and Oceania: 1,659). On the other hand,

505 DQM was the least chosen method across all continents. For QDM, although it was the second
506 most selected method across all continents except South America, the difference in the number
507 of grid points between QDM and EQM is significant.

(a) North America (b) South America (c) Africa (d) Asia (e) Oceania
● EQM ● DQM ● QDM
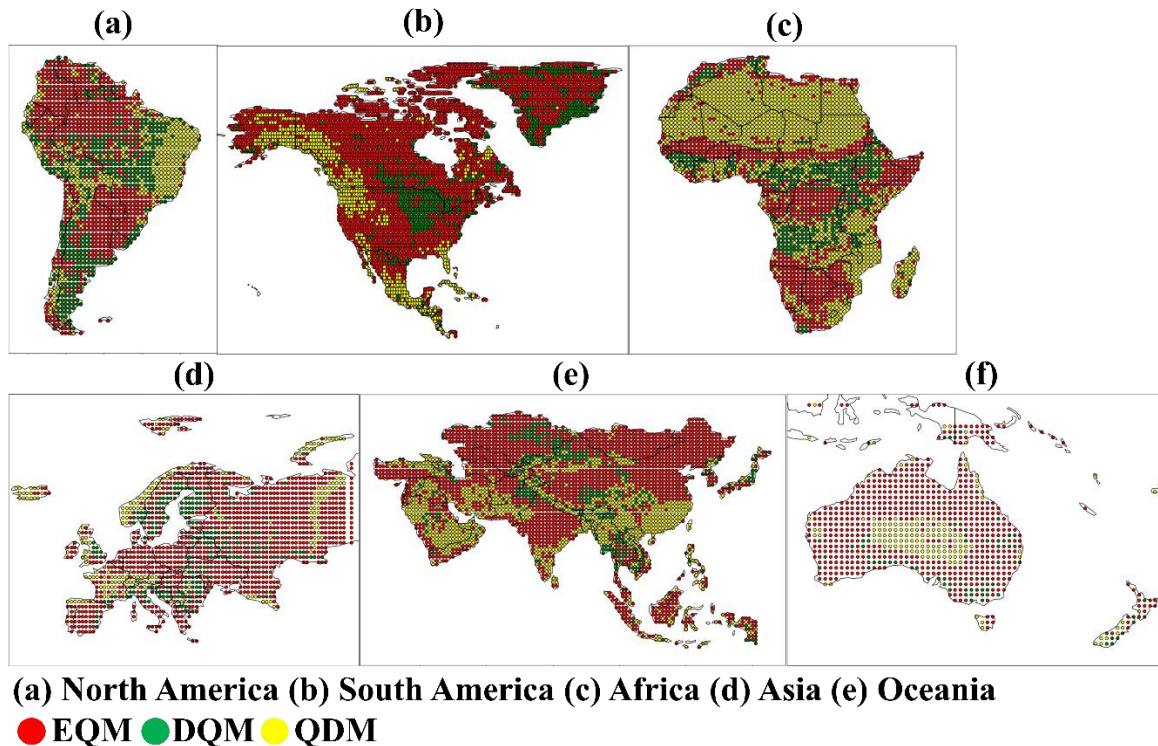
508

509 Figure 11 Spatial distribution for selected best bias correction methods across continents

510 using TOPSIS

511

512 **3.3 Uncertainty quantification of bias corrected daily precipitation**

513 **3.3.1 Uncertainty by model**

514 This study quantifies the daily precipitation uncertainty of 11 CMIP6 GCMs, corrected using

515 three different BMA methods. Figure 12 shows the distribution of GCM weight variances

516 calculated by BMA across six continents. In South America, the highest weight variance was

517 observed mainly in DQM. EQM showed high weight variance in the northern region but lower

518 variance than DQM in most other regions. QDM exhibited the lowest weight variance, with

519 values less than 0.00113 in most regions. In North America, EQM had the lowest weight

520 variance, with values between 0.00055 and 0.00024 in most regions. QDM showed the lowest

521 model uncertainty across North America, with more regions where weight variances were

522 closer to 0 than the other methods. On the other hand, DQM exhibited high weight variance

523 overall, with exceptionally high model uncertainty in the northeast and southern regions. In

524   Africa, EQM's weight variance was estimated to be low overall, resulting in low model

525   uncertainty in most regions. For QDM, weight variance was low in some regions but higher

526   than 0.00113 in others. DQM showed high weight variance in most regions except for the

527   northern area, indicating high model uncertainty across the continent. EQM's weight variance

528   was the lowest in Europe compared to the other methods, with weight variances close to 0

529   across the continent. QDM also showed low weight variance overall, though higher than EQM.

530   DQM exhibited high weight variance in most regions except for Central Europe. In Asia, EQM

531   showed low weight variance in most regions except Southeast Asia. QDM's weight variance

532   was similar to EQM's, though some regions had higher model uncertainty. DQM showed high

533   weight variance in most regions except for some Southwest and North Asian areas. For Oceania,

534   the weight variances of EQM and DQM were mainly similar, but DQM showed a higher weight

535   variance overall.
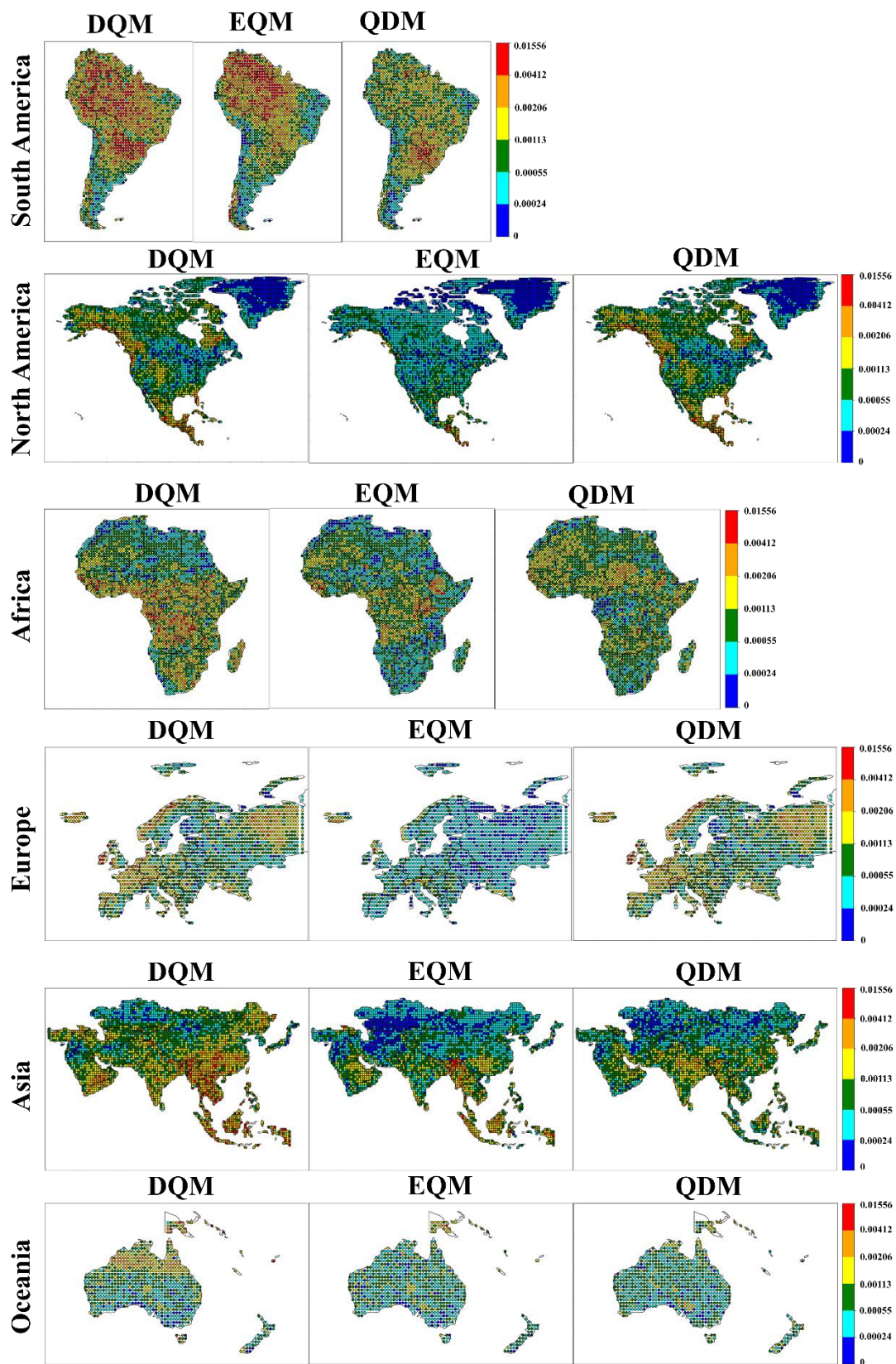
536

537   Figure 12. Spatial distribution of weight variance across continents for bias corrected CMIP6

538   GCMs using BMA

539 Figure 13 shows the distribution of GCM weight variances calculated using BMA across six
540 continents, presented as boxplots. Overall, EQM has the smallest weight variance, and QDM
541 has the second smallest weight variance on all continents except South America. In contrast,
542 in South America, QDM has the smallest weight variance, and EQM has the second smallest.
543 DQM consistently has the largest weight variance across all continents, indicating the highest
544 model uncertainty.
545
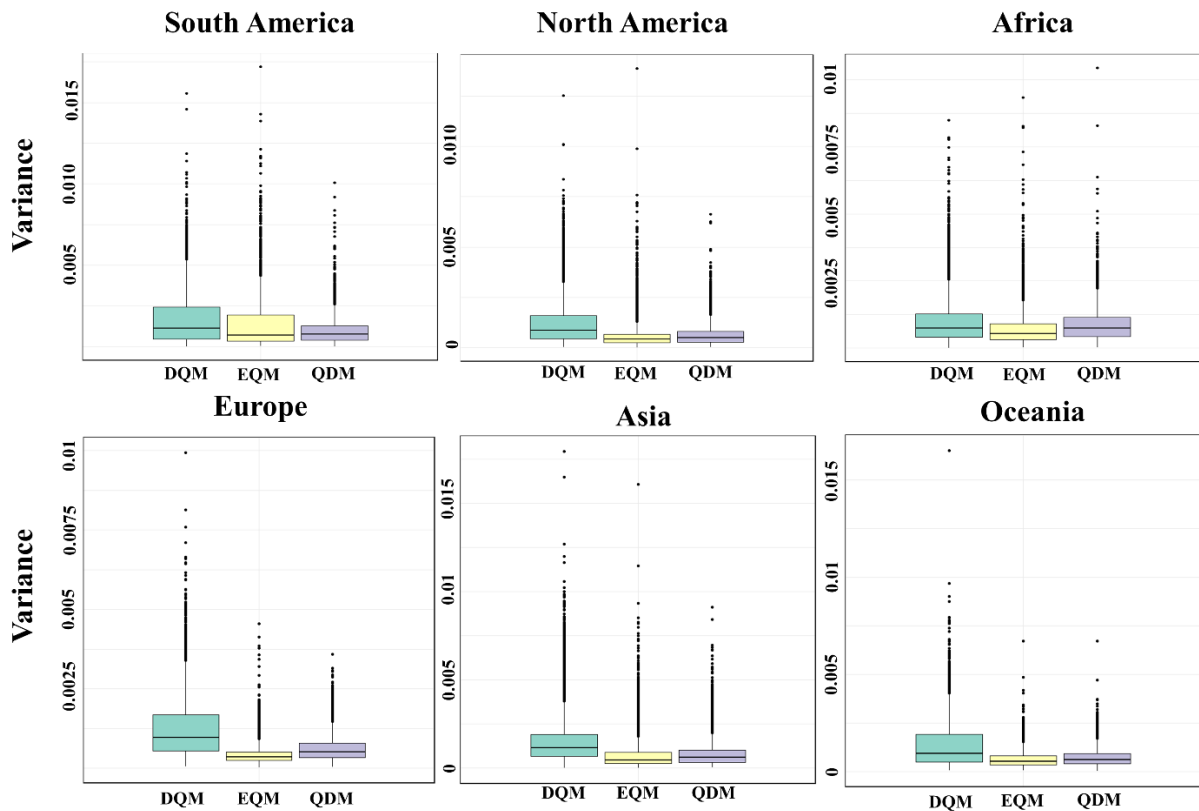
546
547 Figure 13. Weight variance for bias correction methods across six continents using box plots.
548
549 **3.3.2 Uncertainty by ensemble prediction**
550 This study developed a daily precipitation ensemble for the historical period based on 11
551 CMIP6 GCMs using BMA. Figure 14 shows the standard deviation of daily precipitation for
552 the historical period by continent for the ensemble developed using BMA with 11 CMIP6
553 GCMs. Overall, the ensemble predicted using EQM provided stable precipitation projection
554 with low standard deviations across most continents. The QDM ensemble showed similar
555 results to EQM for most continents except Oceania, but the standard deviations were slightly
556 higher. On the other hand, the ensemble using DQM exhibited higher standard deviations than

557   the other methods for all continents and had the largest prediction uncertainty. In Oceania, the

558   ensembles predicted by the three methods showed similar results. However, the prediction

559   uncertainty was estimated to be lower in the order of EQM, DQM, and QDM due to slight

560   differences.
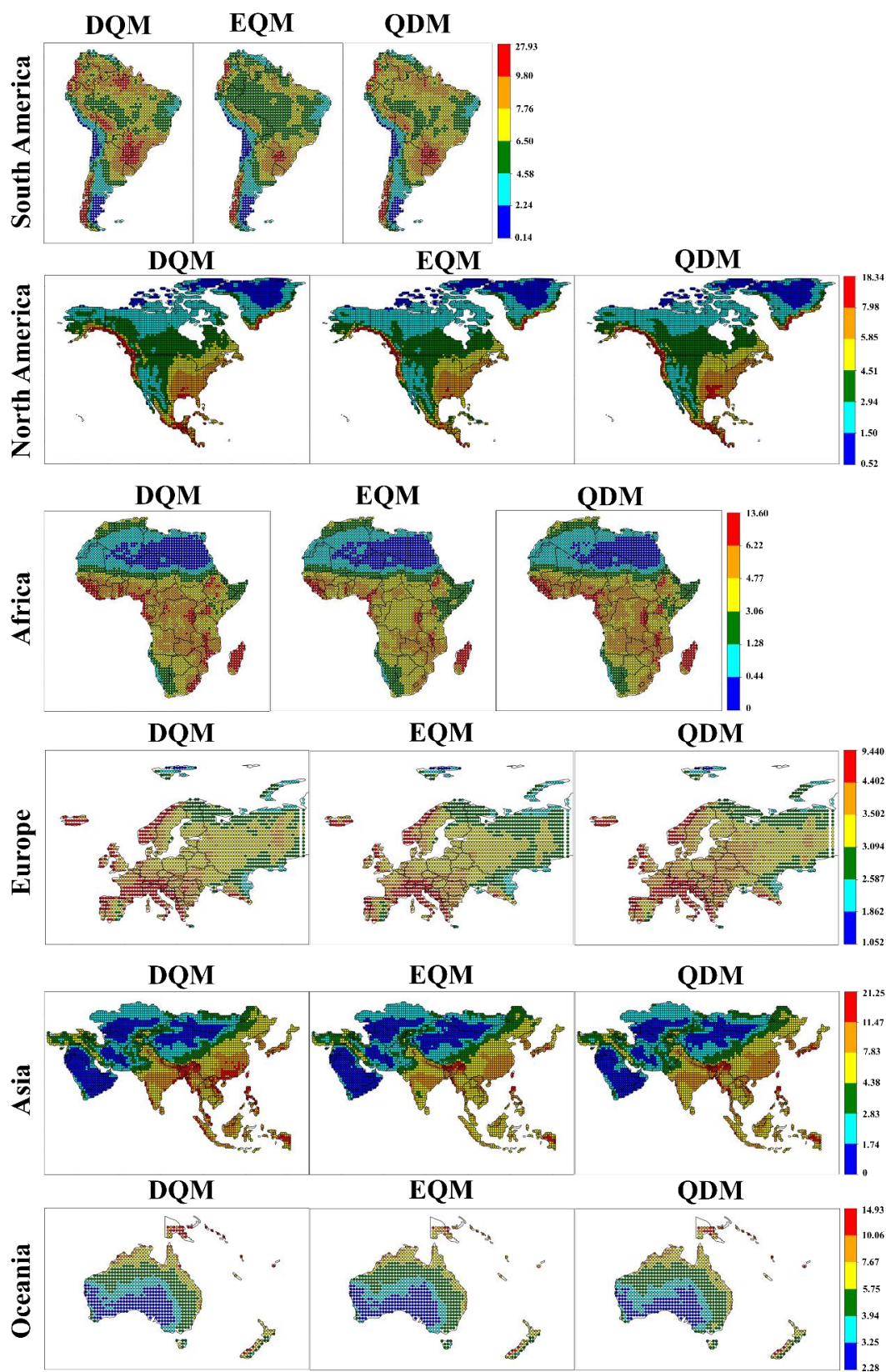
561

562 Figure 14. Spatial distribution of standard deviation for daily precipitation across continents

563 for bias corrected CMIP6 GCMs using BMA

564

565 Figure 15 shows the standard deviation of daily precipitation for the ensemble forecasted by

566 BMA using three methods, DQM, EQM, and QDM, in a boxplot for each continent. Overall,

567 the EQM ensemble showed the lowest standard deviation across all continents, providing the

568 most stable daily precipitation forecasts. The QDM ensemble showed slightly higher standard

569 deviations than EQM for most continents, but there was no significant difference between the

570 two methods. In contrast, the DQM ensemble showed the highest standard deviation and the

571 largest prediction uncertainty.

572

573
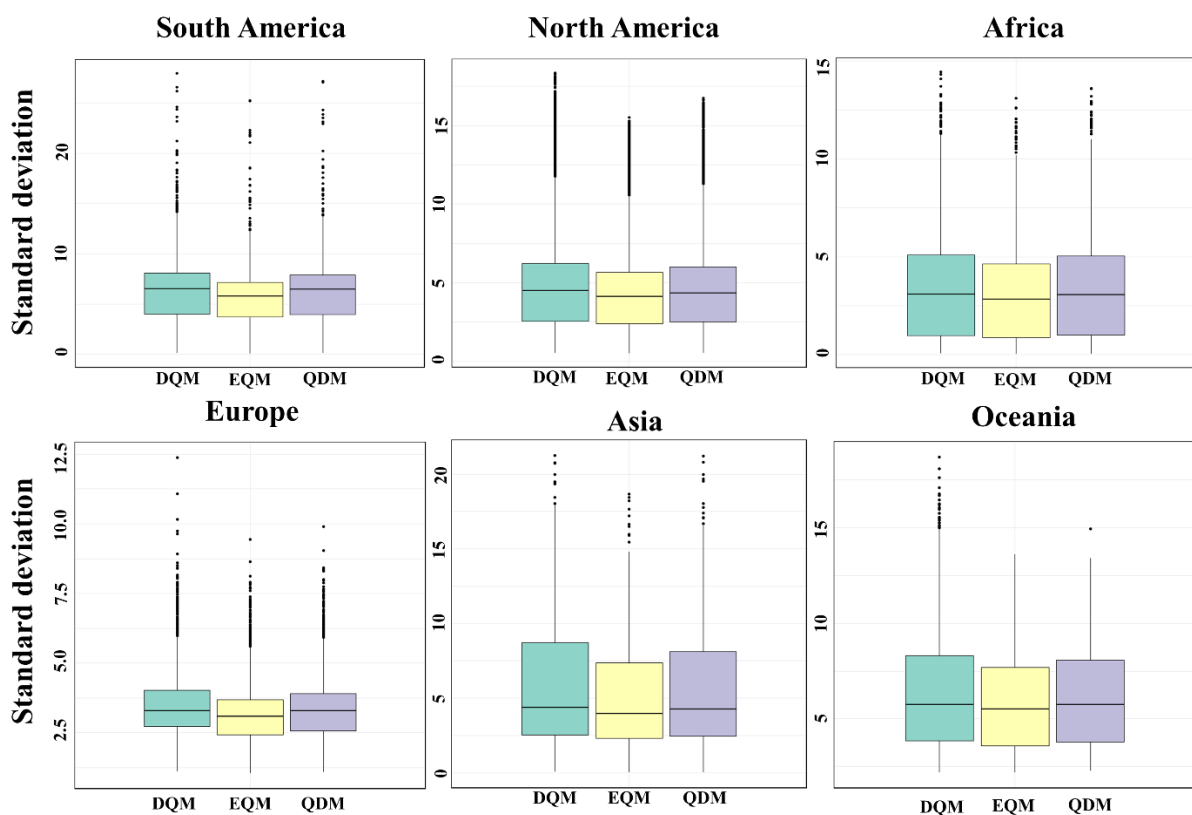
574 Figure 15. Spatial distribution of standard deviation for daily precipitation across continents

575 for bias corrected CMIP6 GCMs using BMA

576

577 **3.4 Evaluation of bias correction methods using CI**

578 **3.4.1 Results of CI by each weighting case**

579 This study compared three QM methods by generating a CI based on three cases of weighting

580 values that considered both model performance and uncertainty. Figures 16, S8, and S9 show

581   the comprehensive indices calculated by applying equal weights and weights emphasizing

582   performance and uncertainty, respectively.

583   EQM showed the highest CI across all continents when equal weights were applied. However,

584   the index was lower in southern Europe and southeastern North America, but it calculated high

585   values in most other regions. QDM showed high index values in some regions, although they

586   were lower than those of EQM. For example, the CI results were high in the northern and

587   western parts of North America and the central part of Europe. On the other hand, DQM was

588   generally unsuitable in most regions but showed a relatively high index in Oceania.

589   When weights that emphasized performance were applied, DQM showed a high index in the

590   central part of South America but low performance in most continents. Nevertheless, DQM

591   showed a better index than QDM in some parts of Oceania. EQM showed the best index across

592   most continents. While QDM was less suitable than EQM, it was still evaluated as a useful

593   method in some continents.

594   Even when applying weights that increased the emphasis on uncertainty, similar results were

595   obtained with the other weighting values. In particular, EQM was evaluated as the most suitable

596   model across all continents, while DQM showed the opposite results.

597
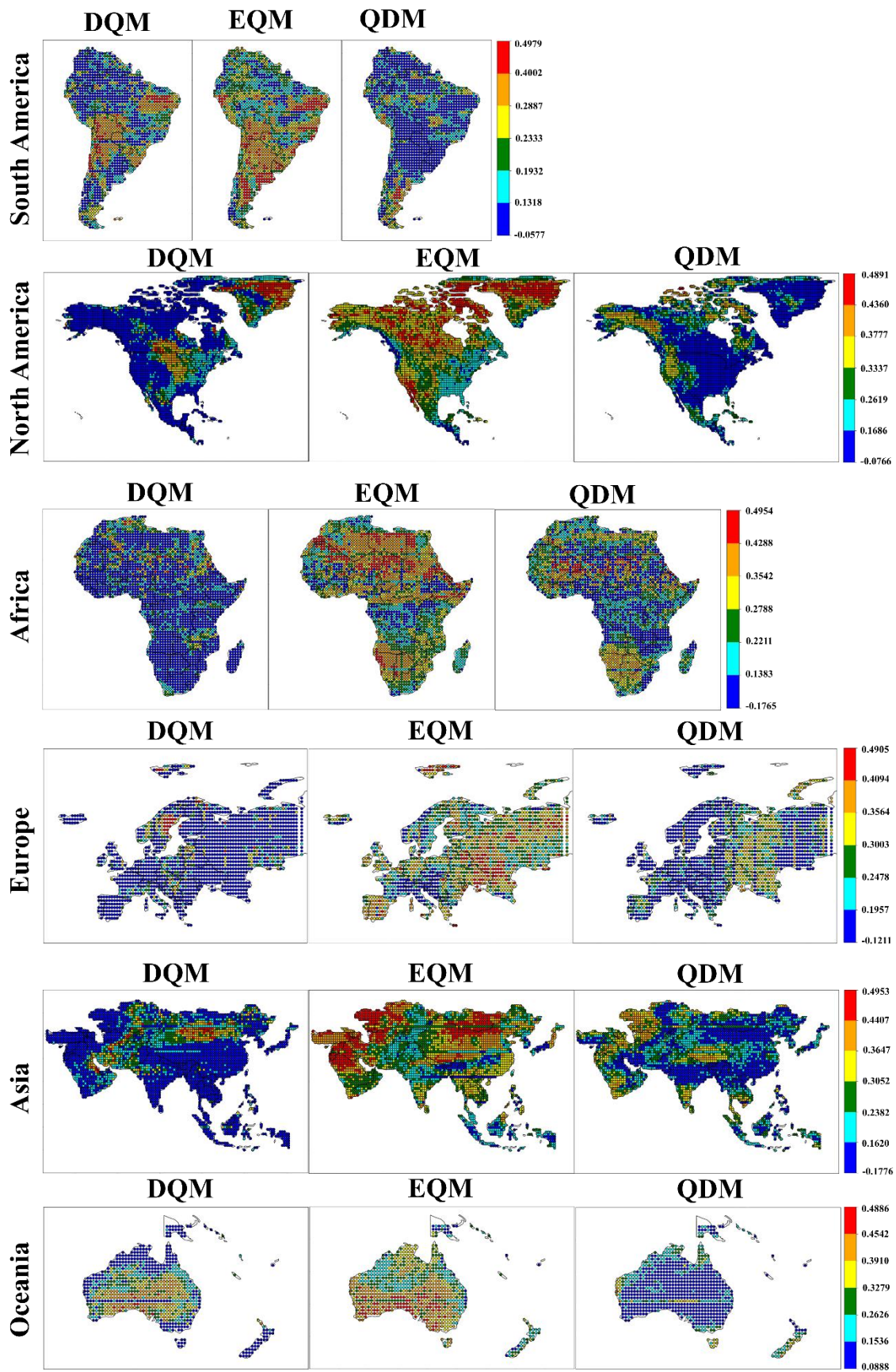
598   Figure 16. Spatial distribution of comprehensive indices for bias correction methods with equal

599   weights (α: 0.5, β: 0.5) across continents

600

601   Figure 17 presents a comparison of the comprehensive indices for three QM methods with

602   different weights for each continent using box plots. Overall, all methods showed higher

603   indices than the other weighting values in the values that emphasized more weight on

604   performance. In all weighted values, DQM showed the lowest indices in all continents except

605   for South America and Oceania, where it was slightly higher or similar to QDM. EQM showed

606   the best composite indices in all continents, outperforming performance and uncertainty. QDM

607   showed high comprehensive indices in most continents, and the gap with EQM narrowed

608   significantly in the weighting values that emphasized performance more. Nevertheless, QDM

609   overall had lower comprehensive indices than EQM.

610
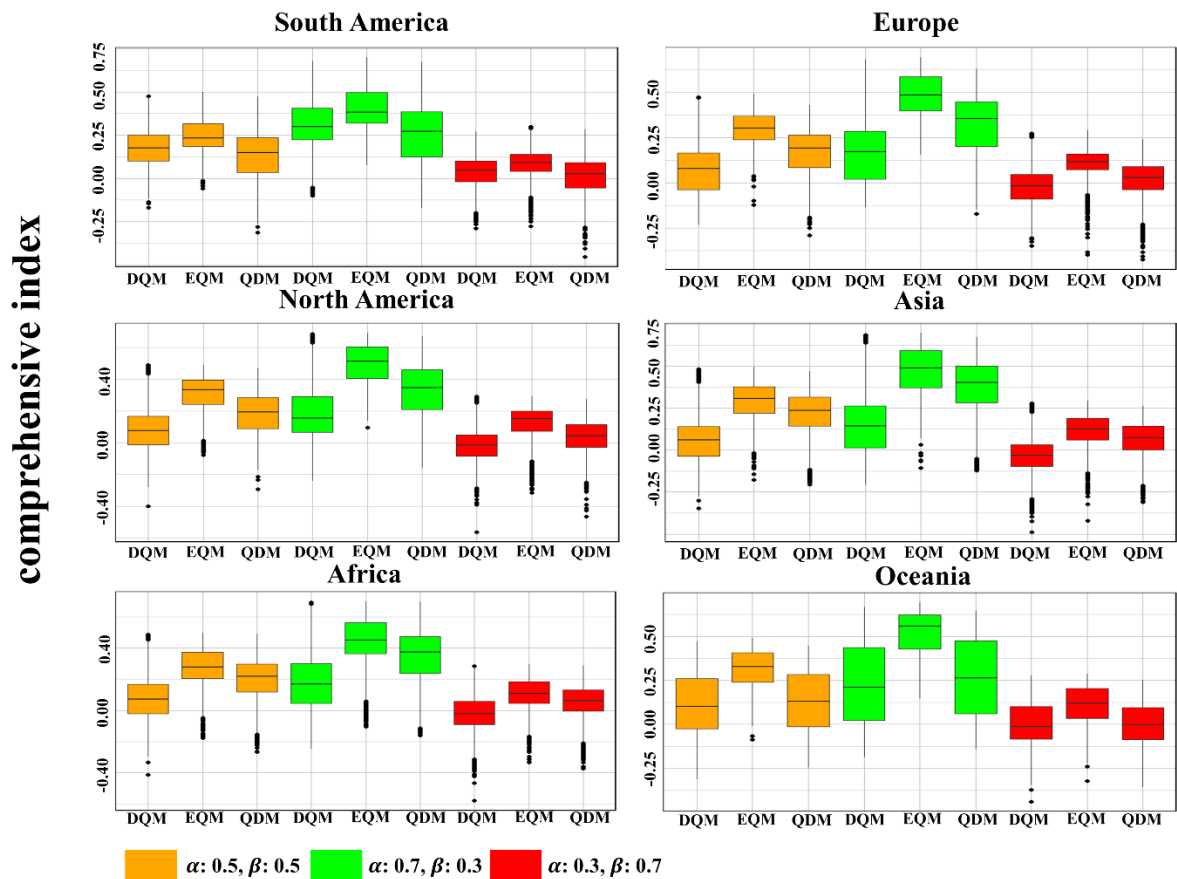
611

612   Figure 17. CI for three bias correction methods across continents with varying weights on

613   performance and uncertainty

614

3.4.2 Selection of best bias correction method

Based on the CI, this study selected the best bias correction method for each continent. Figure 18 shows how the best bias correction method was selected for each continent by applying various weighting values of the CI. Overall, EQM was selected as the best correction method for most continents in all weighting values and was selected more than other methods in North America, Europe, Asia, and Oceania. DQM was selected the least in most continents except for South America and Oceania, and the number of selected grids tended to decrease as the weighting for uncertainty increased. QDM was selected as the proper bias correction method in western North America, southern and eastern Africa, and northern Europe. In addition, QDM was selected the most in Southeast Asia in all weighting values.
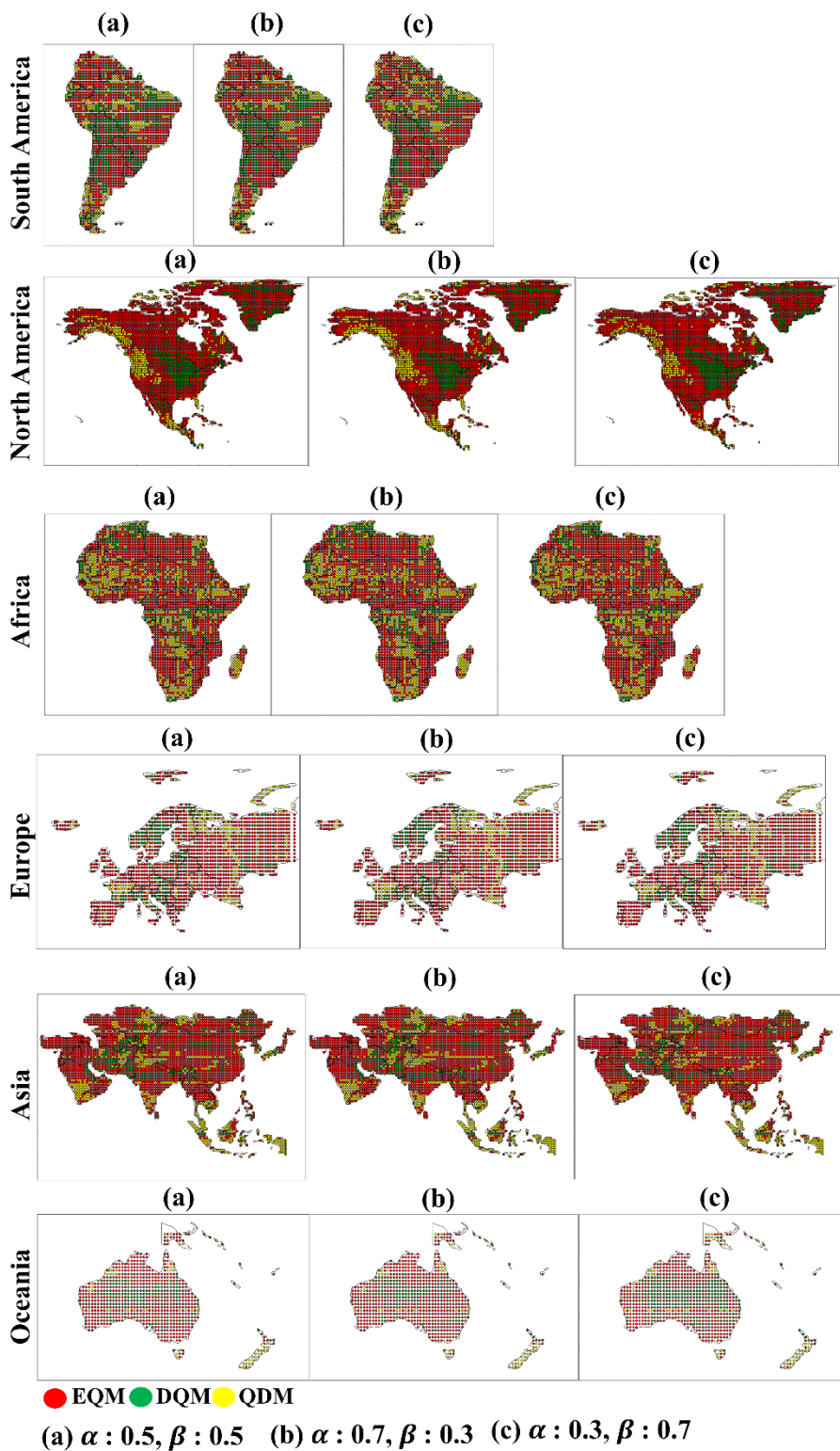
626   Figure 18. Selection of best bias correction methods across continents based on CI depending

627   on weighting values.

628

629 Figure 19 shows the number of selected grids for the best bias correction method across
630 continents based on three weighting values. Overall, EQM was the most frequently selected
631 method across all weighting values, demonstrating superior performance across all continents
632 compared to the other methods. Interestingly, as the weight for uncertainty increased, the
633 number of grids where EQM was selected also increased, while the number decreased as the
634 weight for performance increased. In contrast, QDM was chosen as the second-best method on
635 most continents, except for South America and Oceania. The number of selected grids for
636 QDM slightly increased as the performance weight increased. DQM was the least selected
637 method across most continents, indicating that it was the least suitable overall.

638
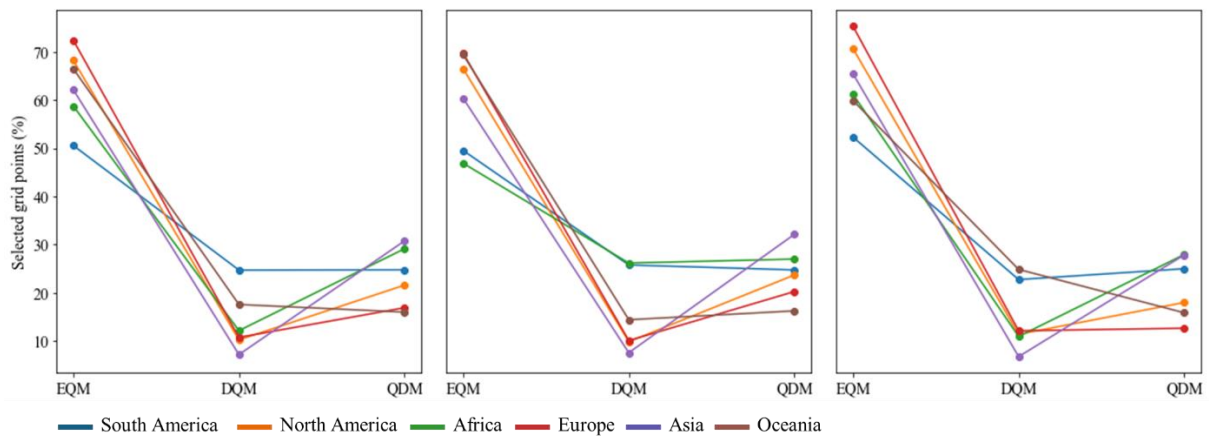
639

640 Figure 19. Ratios of selected grids for best bias correction methods across continents based on
641 different weighting values

642

643 **4. Discussion**

644 Bias correction methods are widely used in correcting GCM outputs, and previous studies have
645 compared the performance of various methods (Homsi et al., 2019; Saranya and Vinish, 2021).
646 Among these, Quantile Mapping (QM) has consistently shown superior performance compared
647 to other methods, making it a widely used approach for bias correction. In particular, QDM,
648 EQM, and DQM, which are the focus of this study, are frequently employed in research
649 exploring and applying climate change projections based on GCM outputs (Cannon et al., 2015;
650 Switanek et al., 2016; Song et al., 2022a). Analyzing the strengths and limitations of these three
651 methods will provide valuable insights for climate researchers, enabling them to choose the
652 most suitable bias correction method for specific regions. In this context, this study further
653 evaluates the performance of QDM, EQM, and DQM, especially for daily precipitation, and

investigates how these methods perform across different regions. Unlike previous studies that focused on the performance of bias correction methods (Song et al., 2024a; Teutschbein and Seibert, 2012; Smitha et al., 2018), this study suggests a CI that integrates the performance and uncertainty metrics. This approach enhances the robustness of bias correction method selection and provides a more holistic evaluation framework. This section discusses the strengths and weaknesses of each method from various perspectives to provide a more balanced assessment.

4.1 Evaluation of bias correction methods performance

The daily precipitation corrected by the three QM methods outperformed the raw GCM data (see Figure 1). All three methods showed strong overall performance, as indicated by the Taylor diagram, producing consistently good results across different regions. This highlights the need to use multiple performance metrics to fully understand the strengths and weaknesses of the three QM methods, as relying on a single analysis or macroscopic perspective can overlook important details. From this perspective, many studies have emphasized the application of a multifaceted analysis in selecting bias correction methods (Homsi et al., 2019; Cannon et al., 2015; Berg et al., 2022; Song et al., 2023). The spatial distribution of correction performance, as discussed in Section 3.1.2, varies significantly by continent. Figures 2 to 7 reveal that the evaluated metrics differ across continents, underscoring the importance of region-specific correction methods. This finding aligns with Song et al. (2023), highlighting the importance of selecting appropriate correction methods based on the precipitation distribution at observation sites. Moreover, studies such as Homsi et al. (2019) and Saranya and Vinish (2021) also emphasize the variability in bias correction performance depending on the regional climate and data characteristics, reinforcing the need for tailored approaches. Of course, the three QM methods showed high performance across most continents, effectively correcting the biases in daily precipitation from GCMs. However, the corrected daily precipitation varies subtly among the three methods, with these differences becoming more pronounced in extreme events or specific evaluation metrics. For example, the three QM methods tend to perform less effectively in regions with high precipitation, but their performance also varies by grid (e.g., southern India in Asia: RMSE; central Oceania: Pbias and EVS; central Europe: Pbias, MdAE, and KGE). While EQM performs well across most continents, DQM and QDM show superior results in specific regions. Similar results were made by Cannon et al. (2015), which highlighted differences in the performance of bias

correction methods, particularly in handling extreme precipitation events. QDM's error-related metrics (South America: RMSE, MAE, and MSLE) are nearly identical to EQM's, yet QDM outperforms EQM regarding MdAE on more grids. These findings suggest that a more nuanced and detailed analysis of precipitation corrected by GCMs is necessary, aligning with the conclusions of Gudmundsson et al. (2012), which emphasize that the effectiveness of bias correction methods can vary significantly depending on local climate characteristics, highlighting the importance of selecting appropriate methods for each region. These results suggest a more detailed precipitation analysis from corrected GCMs is needed.

This study compared the three QM methods for daily precipitation events above the 95th percentile (extreme precipitation) using the GEV distribution, as shown in Figure 10. The results indicate that DQM tends to correct more extreme precipitation events than QDM, aligning with previous findings that DQM captures a broader range of extremes. The unique characteristics of DQM caused these results. DQM overestimated the corrected extreme precipitation due to the relative variability in the data introduced through detrending, and the subsequent reintroduction of the long-term mean during the correction step widened the range of extreme precipitation, leading to overestimation compared to the reference data in areas with high variability. At the same time, QDM and EQM take a more conservative approach (as noted in previous studies such as Cannon et al., 2015). These findings suggest that EQM and QDM may be more suitable in regions vulnerable to floods and extreme weather events that require a more balanced and cautious approach. However, when comparing the differences in GEV distributions, there was no significant difference between methods in regions like Oceania and Europe (see Figure 9). These results imply that EQM can better handle extreme values or outliers in the data by directly comparing and correcting past and future distributions. In particular, EQM is consistent with previous studies in that it more accurately corrects observed distributions in non-stationary and highly variable climate variables, such as precipitation (Themeßl et al., 2012; Maraun, 2013; Gudmundsson et al., 2012). These positive aspects are mainly due to EQM's ability to align the empirical ECDFs of reference and model data across all quantiles, allowing it to correct biases with high precision at both central tendencies and extremes. Although there are significant advantages in observing the results of the correction method in detail from various perspectives, presenting these results without integrating them into a reasonable framework can increase confusion and uncertainty in climate change research

717   (Wu et al., 2022). Therefore, it is essential to introduce a structured framework such as MCDA

718   to provide a single integrated result.

719

720   **4.2 Uncertainties of model and ensemble prediction in bias correction methods**

721   In climate modeling, quantifying uncertainty is essential to assess the reliability of bias-

722   corrected precipitation data. This study applied BMA to quantify the uncertainty of three QM

723   methods on a continental basis, addressing both model-specific and ensemble prediction

724   uncertainties. Similar to the findings by Cannon et al. (2015), this analysis demonstrates how

725   different bias correction methods yield varying uncertainty levels based on the underlying

726   climate models. Notably, EQM showed the lowest weight variance across most continents,

727   which means that the inter-model uncertainty for 11 GCMs corrected by EQM is lower than

728   that of the other QM methods. The low uncertainty associated with EQM aligns with previous

729   studies like Themeßl et al. (2012), which found that EQM consistently reduced discrepancies

730   between modeled and observed data across regions. EQM's ability to manage extreme

731   precipitation and anomalous values based on observed distributions contributes to its reliability,

732   a feature also emphasized by Gudmundsson et al. (2012). On the other hand, DQM showed the

733   highest weight variance across all continents, indicating more significant uncertainty when

734   applied to various GCMs. This uncertainty was particularly pronounced in regions with

735   complex climate conditions, such as Southeast Asia, East Africa, and the Alps in Europe. These

736   results align with Berg et al. (2022), who highlighted DQM's limitations in capturing long-term

737   climate trends and extreme events. The higher uncertainty associated with DQM suggests that,

738   while its detrending process is effective in correcting the mean, it may struggle in regions

739   dominated by nonlinear climate patterns, as it does not sufficiently account for all quantiles in

740   the distribution, particularly extremes, as noted by Cannon et al. (2015). QDM, though showing

741   lower weight variance than DQM, still demonstrated higher uncertainty than EQM in regions

742   with diverse climate characteristics. These results are consistent with the study of Tong et al.

743   (2021), suggesting that QDM performs better under moderate precipitation scenarios. However,

744   the uncertainty may increase under highly variable or extreme weather conditions. Furthermore,

745   this study extended the uncertainty analysis to ensemble predictions, calculating the standard

746   deviation of daily precipitation for each continent using BMA. The EQM-based ensemble

747   consistently exhibited low standard deviations across all continents, indicating that EQM offers

748   the most stable and reliable precipitation predictions. This finding echoes the conclusions

749 drawn by Teng et al. (2015), where EQM provided more accurate and less uncertain projections.
750 In contrast, DQM presented the most significant prediction uncertainty, reinforcing the need
751 for caution when applying DQM in studies that require high-confidence data. These results
752 emphasize the importance of weighing performance and uncertainty when choosing a suitable
753 bias correction method. EQM's consistent performance in reducing uncertainty across model-
754 specific and ensemble forecasts highlights its robustness as a preferred choice for climate
755 research. However, the substantial uncertainty associated with DQM suggests that its use
756 should be limited to regions where its detrending process can be beneficial. Overall, these
757 findings stress the critical role of uncertainty quantification in climate change impact
758 assessments and underscore the need for selecting bias correction methods based on a
759 comprehensive evaluation of both performance and uncertainty.
760

761 **4.3 Integrated assessment of bias correction methods**
762 This study selected the optimal QM method for each continent based on the CI, which considers
763 uncertainty and performance. The critical point is that uncertainty is decisive when selecting a
764 bias correction method. As shown in Figure 19, the optimal correction method varies depending
765 on the continent, and the selected method also changes depending on the weight. These results
766 suggest that uncertainty still exists, as Berg et al. (2022) pointed out, and that uncertainty must
767 be considered when selecting the optimal method. In other words, even if the QM method has
768 high performance, it is difficult to make a reasonable selection if the uncertainty contained in
769 the method is significant. Overall, EQM showed the highest CI value in all continents, which
770 means that it provides the most balanced results in terms of performance and uncertainty. These
771 results are consistent with previous studies (Lafon et al., 2013; Teutschbein and Seibert, 2012;
772 Teng et al., 2015) that showed high precipitation correction accuracy and excellent
773 performance, especially under complex climate conditions. QDM was evaluated highly in some
774 regions but performed worse than EQM overall. Berg et al. (2022) also pointed out that QDM
775 is superior in general climate conditions but may perform worse in extreme climate situations,
776 suggesting that this may increase the uncertainty of QDM in extreme climates. DQM was
777 evaluated as an unsuitable method in most regions due to low CI values, which is consistent
778 with the limitations of DQM mentioned in Cannon et al. (2015) and Berg et al. (2022). It was
779 confirmed that DQM performs relatively well in dry climates but may perform worse in various
780 climate conditions. In addition, some differences were observed with the results based on

TOPSIS. For example, DQM was selected more than QDM in South America, but when the uncertainty weight was applied, QDM was selected more. Conversely, in Oceania, QDM was selected more than DQM, but when the uncertainty weight was increased to 0.7, DQM was selected more. These results are consistent with those of Lafferty and Sriver (2023), showing that when significant uncertainty exists, uncertainty can be greater despite high bias correction performance. In conclusion, EQM is the most balanced method regarding performance and uncertainty and will likely be preferred in future climate modeling studies. However, there may be more suitable QM methods depending on the region, and a comprehensive evaluation with various weights is needed. Therefore, when establishing climate change response strategies or policy decisions, it is essential to take a multifaceted approach that considers uncertainty together rather than relying on a single indicator or performance alone. It will enable more reliable predictions and better decision-making.

5. Conclusion

This study corrected and compared historical daily precipitation from 11 CMIP6 GCMs using three QM methods. Eleven statistical metrics were used to evaluate the precipitation performance corrected by three QM methods, and TOPSIS was applied to select performance-based priorities. BMA was applied to quantify model-specific and ensemble prediction uncertainties. Additionally, suitable QM methods were selected and compared using a CI that integrates TOPSIS performance scores with BMA uncertainty metrics. The conclusions of this study are as follows:

1. EQM showed the highest overall index across all continents, indicating that it provides the most balanced approach in terms of performance and uncertainty.

2. DQM effectively reproduced the dry climate in North Africa and parts of Central and Southwest Asia but showed the highest uncertainty across all continents. These results suggest that DQM may lose some long-term trend information, making it less reliable in regions prone to extreme weather events.

3. QDM performed better in certain regions, such as Southeast Asia, and was selected more often than DQM when uncertainty was given greater weight. QDM may be a promising alternative in areas where uncertainty plays a significant role.

811   4. Selecting an appropriate QM is required for high performance, and significant
812   uncertainty can complicate rational decision-making. Therefore, a multifaceted
813   approach considering performance and uncertainty is essential in climate modeling.

814 In conclusion, EQM has emerged as the preferred method due to its balanced performance, but
815 this study emphasizes the importance of regional assessment and careful consideration of
816 uncertainty when selecting a QM method. Future research should integrate greenhouse gas
817 scenarios to improve the accuracy of climate predictions and provide a more comprehensive
818 understanding of future climate risks. Based on the results of this study, future studies can
819 develop hybrid methodologies that combine the strengths of each QM.

820

Code availability

822 Codes for benchmarking the xclim of python package are available from
823 https://doi.org/10.5281/zenodo.10685050 (Bourgault et al., 2024). Furthermore, the CI
824 proposed in this study, along with the TOPSIS and BMA used within it, is available at
825 https://doi.org/ 10.5281/zenodo.14351816 (Song, 2024b).

826

Data availability

828 The data used in this study are publicly available from multiple sources. CMIP6 General
829 Circulation Models (GCMs) outputs were obtained from the Earth System Grid Federation
830 (ESGF) data portal at https://esgf-node.llnl.gov/search/cmip6/. Users can select data types such
831 as climate variables, time series, and experiment ID, which can be downloaded as NC files.
832 Furthermore, CMIP6 GCMs output can also be accessed in Eyring et al. (2016) The ERA5
833 reanalysis dataset used in this study is available through the Copernicus Data Store (CDS)
834 provided by ECMWF (https://cds.climate.copernicus.eu/cdsapp#!/dataset/reanalysis-era5-
835 single-levels?tab=overview). ERA5 is available at https://doi.org/10.24381/cds.bd0915c6
836 (Hersbach et al., 2023). The daily precipitation datasets from CMIP6 GCM and ERA5 used in
837 this study are available at https://doi.org/10.6084/m9.figshare.27999167.v5 (Song, 2024c).

838

Author contributions

840 Young Hoon Song: Conceptualization, Methodology, Data curation, Funding acquisition,
841 Visualization, Writing – original draft, Writing – review & editing. Eun Sung Chung: Formal

842   analysis, Funding acquisition, Methodology, Project administration, Supervision, Validation,

843   Writing-review & editing

844

845   **Declaration of Competing Interests**

846   The authors declare that they have no known competing financial interests or personal

847   relationships that could have appeared to influence the work reported in this paper.

848

849   **Acknowledgement**

850   This study was supported by National Research Foundation of Korea (NRF) (RS-2023-

851   00246767_2; 2021R1A2C200569914)

852

853   **Reference**

854   1.   Abdelmoaty, H.M., and Papalexiou, S.M.: Changes of Extreme Precipitation in

855   CMIP6 Projections: Should We Use Stationary or Nonstationary Models? J. Clim.

856   36(9), 2999-3014, https://doi.org/10.1175/JCLI-D-22-0467.1, 2023.

857   2.   Ansari, R., Casanueva, A., Liaqat, M.U., and Grossi, G.: Evaluation of bias

858   correction methods for a multivariate drought index: case study of the Upper Jhelum

859   Basin. GMD 16(7), 2055-2076, https://doi.org/10.5194/gmd-16-2055-2023, 2023.

860   3.   Berg P., Bosshard, T., Yang, W., and Zimmermann, K.: MIdASv0.2.1 – MultI-scale

861   bias AdjuStment. GMD 15, 6165-6180, https://doi.org/10.5194/gmd-15-6165-2022,

862   2022

863   4.   Bourgault, P., Huard, D., Smith, T.J., Logan, T., Aoun, A., Lavoie, J., Dupuis, É.,

864   Rondeau-Genesse, G., Alegre, R., Barnes, C., Beaupré Laperrière, A., Biner, S.,

865   Caron, D., Ehbrecht, C., Fyke, J., Keel, T., Labonté, M.P., Lierhammer, L., Low,

866   J.F., Quinn, J., Roy, P., Squire, D., Stephens, Ag., Tanguy, M., Whelan, C., Braun,

867   M., Castro, D.: xclim: xarray-based climate data analytics (0.48.1). Zenodo [Code],

868   https://doi.org/10.5281/zenodo.10685050, 2024.

869   5.   Cannon, A. J., Sobie, S. R., and Murdock, T.Q.: Bias correction of GCM

870   precipitation by quantile mapping: How well do methods preserve changes in

871   quantiles and extremes? J. Clim. 28(17), 6938-6959, https://doi.org/10.1175/JCLI-D-

872   14-00754.1, 2015.

873   6.   Cannon, A.J.: Multivariate quantile mapping bias correction: an N-dimensional

874   probability density function transform for climate model simulations of multiple

875   variables. Clim. Dyn. 50, 31–49. https://doi.org/10.1007/s00382-017-3580-6, 2018.

876   7. Chae, S. T., Chung, E. S., and Jiang, J.: Robust siting of permeable pavement in

877   highly urbanized watersheds considering climate change using a combination of

878   fuzzy-TOPSIS and the VIKOR method. Water Resour. Manag. 36(3), 951–969,

879   https://doi.org/10.1007/s11269-022-03062-y, 2022.

880   8. Chua, Z.W., Kuleshov, Y., Watkins, A.B., Choy, S., and Sun, C.: A Comparison of

881   Various Correction and Blending Techniques for Creating an Improved Satellite-

882   Gauge Rainfall Dataset over Australia. Remote Sens, 14(2), 261,

883   https://doi.org/10.3390/rs14020261, 2022.

884   9. Chung, E. S., and Kim, Y.J.: Development of fuzzy multi-criteria approach to

885   prioritize locations of treated wastewater use considering climate change scenarios.

886   JEM 146, 505–516, https://doi.org/10.1016/j.jenvman.2014.08.013, 2014.

887   10. Cox, P., and Stephenson, D.: A changing climate for prediction. Science 317(5835),

888   207–208, https://www.science.org/doi/10.1126/science.1145956, 2007.

889   11. Deser, C., Phillips, A., Bourdette, V., and Teng, H.: Uncertainty in climate change

890   projections: the role of internal variability. Clim. Dyn. 38, 527–546,

891   https://doi.org/10.1007/s00382-010-0977-x, 2012

892   12. Déqué, M.: Frequency of precipitation and temperature extremes over France in an

893   anthropogenic scenario: Model results and statistical correction according to

894   observed values. Glob. Planet. Change. 57(1-2), 16-26,

895   https://doi.org/10.1016/j.gloplacha.2006.11.030, 2007.

896   13. Ehret, U., Zehe, E., Wulfmeyer, V., Warrach-Sagi, K., and Liebert, J.: HESS

897   Opinions "Should we apply bias correction to global and regional climate model

898   data?". HESS 16(9), 3391-3404, https://doi.org/10.5194/hess-16-3391-2012, 2012.

899   14. Enayati, M., Bozorg-Haddad, O., Bazrafshan, J., Hejabi, S., and Chu, X.: Bias

900   correction capabilities of quantile mapping methods for rainfall and temperature

901   variables. Water and Climate change 12(2), 401-419,

902   https://doi.org/10.2166/wcc.2020.261, 2021.

903   15. Evin, G., Ribes, A., and Corre, L.: Assessing CMIP6 uncertainties at global warming

904   levels. Clim Dyn. https://doi.org/10.1007/s00382-024-07323-x, 2024.

905   16. Eyring, V., Bony, S., Meehl, G., Senior, C., Stevens, B., Stouffer, R., and Taylor, K.:

Overview of the Coupled Model Intercomparison Project Phase 6 (CMIP6) experimental design and organization. Geoscientific Model Development, 9(5), 1937–1958. 2016. https://doi.org/10.5194/gmd-9-1937-2016

17. Galton, F.: Regression Towards Mediocrity in Hereditary Stature. The Journal of the Anthropological Institute of Great Britain and Ireland 15, 246-263, https://doi.org/10.2307/2841583, 1886.

18. Giorgi, F., and Mearns, L.O.: Calculation of average, uncertainty range, and reliability of regional climate changes from AOGCM simulations via the "reliability ensemble averaging" (REA) method, J. Clim. 15, 1141–1158, https://doi.org/10.1175/1520-0442(2002)015<1141:COAURA>2.0.CO;2, 2000.

19. Gupta, H.V., Kling, H., Yilmaz, K.K., and Martinez, G.F.: Decomposition of the mean squared error and NSE performance criteria: Implications for improving hydrological modelling. J. Hydrol. 377(1–2), 80–91, https://doi.org/10.1016/j.jhydrol.2009.08.003, 2009

20. Gudmundsson, L., Bremnes, J.B., Haugen, J.E., and Engen-Skaugen, T.: Technical Note: Downscaling RCM precipitation to the station scale using statistical transformations – a comparison of methods. HESS 16(9), 3383–3390, https://doi.org/10.5194/hess-16-3383-2012, 2012.

21. Hamed, M.M., Nashwan, M.S., Shahid, S., Wang, X.J., Ismail, T.B., Dewan, A., and Asaduzzaman, M.d: Future Köppen-Geiger climate zones over Southeast Asia using CMIP6 Multimodel Ensemble. Atmos. Res. 283(1), 106560, https://doi.org/10.1016/j.atmosres.2022.106560, 2023.

22. Hersbach, H., Bell, B., Berrisford, P., Hirahara, S., Horányi, A., Muñoz-Sabater, J., Nicolas, J., Peubey, C., Radu, R., Schepers, D., Simmons, A., Soci, C., Abdalla, S., Abellan, X., Balsamo, G., Bechtold, P., Biavati, G., Bidlot, J., Bonavita, M., Chiara, G., Dahlgren, P., Dee, D., Diamantakis, M., Dragani, R., Flemming, J., Forbes, R., Fuentes, M., Geer, A., Haimberger, L., Healy, S., Hogan, R. J., Hólm, E., Janisková, M., Keeley, S., Laloyaux, P., Lopez, P., Lupu, C., Radnoti, G., Rosnay, P., Rozum, I., Vamborg, F., Villaume, S., and Thépaut, J.: The ERA5 global reanalysis, Q. J. Roy. Meteor. Soc., 146, 1999–2049, https://doi.org/10.1002/qj.3803, 2020.

23. Hersbach, H., Bell, B., Berrisford, P., Biavati, G., Horányi, A., Muñoz Sabater, J., Nicolas, J., Peubey, C., Radu, R., Rozum, I., Schepers, D., Simmons, A., Soci, C.,

938   Dee, D., and Thépaut, J.-N.: ERA5 hourly data on pressure levels from 1940 to

939   present, Copernicus Climate Change Service (C3S) Climate Data Store (CDS),

940   https://doi.org/10.24381/cds.bd0915c6, 2023.

941   24. Homsi, R., Shiru, M. S., Shahid, S., Ismail, T., Harun, S. B., Al-Ansari, N., and

942   Yaseen, Z.M: Precipitation projection using a CMIP5 GCM ensemble model: a

943   regional investigation of Syria. Eng. Appl. Comput. Fluid Mech. 14(1), 90–106,

944   https://doi.org/10.1080/19942060.2019.1683076, 2019.

945   25. Hoeting J.A., Madigan D., Raftery A.E., and Volinsky C.T.: BayesIan model

946   averaging: A tutorial (with discussion). Stat. Sci. 214, 382-417,

947   https://doi.org/10.1214/ss/1009212519, 1999.

948   26. Hosking, J.R.M., Wallis, J.R., and Wood, E.F.: Estimation of the generalized

949   extreme value distribution by the method of probability weighted monents.

950   Technometrics 27, 251–261, https://doi.org/10.1080/00401706.1985.10488049,

951   1985.

952   27. Hosking, J.R.M.: L-moments: Analysis and estimation of distributions using linear

953   combinations of order statistics. J. R. Stat. 52, 105–124,

954   https://doi.org/10.1111/j.2517-6161.1990.tb01775.x, 1990.

955   28. Hwang, C. L., and Yoon, K.: Multiple attribute decision making: Methods and

956   applications. Springer-Verlag. https://doi.org/10.1007/978-3-642-48318-9. 1981.

957   29. IPCC: Climate Change 2021: The Physical Science Basis. Contribution of Working

958   Group I to the Sixth Assessment Report of the Intergovernmental Panel on Climate

959   Change, edited by: Masson-Delmotte, V., Zhai, P., Pirani, A., Connors, S. L., Péan,

960   C., Berger, S., Caud, N., Chen, Y., Goldfarb, L., Gomis, M. I., Huang, M., Leitzell,

961   K., Lonnoy, E., Matthews, J. B. R., Maycock, T. K., Waterfield, T., Yelekçi, O., Yu,

962   R., and Zhou, B., Cambridge University Press,

963   https://doi.org/10.1017/9781009157896, 2021.

964   30. IPCC: Climate Change 2022: Impacts, Adaptation, and Vulnerability. Contribution

965   of Working Group II to the Sixth Assessment Report of the Intergovernmental Panel

966   on Climate Change, edited by: Pörtner, H.-O., Roberts, D. C., Tignor, M.,

967   Poloczanska, E. S., Mintenbeck, K., Alegría, A., Craig, M., Langsdorf, S., Löschke,

968   S., Möller, V., Okem, A., and Rama, B., Cambridge University Press,

969   https://doi.org/10.1017/9781009325844, 2022.

970   31. Ishizaki, N.N., Shiogama, H., Hanasaki, N., Takahashi, K., and Nakaegawa, T.:

971   Evaluation of the spatial characteristics of climate scenarios based on statistical and

972   dynamical downscaling for impact assessments in Japan. Int. J. Climatol. 43(2),

973   1179-1192, https://doi.org/10.1002/joc.7903, 2022.

974   32. Jobst, A.M., Kingston, D.G., Cullen, N.J., and Schmid, J.: Intercomparison of

975   different uncertainty sources in hydrological climate change projections for an alpine

976   catchment (upper Clutha River, New Zealand). HESS 22, 3125-3142,

977   https://doi.org/10.5194/hess-22-3125-2018, 2018.

978   33. Lafferty, D.C., and Sriver, R.L.: Downscaling and bias-correction contribute

979   considerable uncertainty to local climate projections in CMIP6. npj Clim Atmos

980   Sci 6, 158, https://doi.org/10.1038/s41612-023-00486-0, 2023.

981   34. Lafon, T., Dadson, S., Buys, G., and Prudhomme, C.: Bias correction of daily

982   precipitation simulated by a regional climate model: a comparison of methods. Int. J.

983   Climatol. 33, 1367-1381, http://dx.doi.org/10.1002/joc.3518, 2013.

984   35. Lin, J.: Divergence measures based on the Shannon entropy. IEEE Transactions on

985   Information Theory 37(1), 145–151, https://doi.org/10.1109/18.61115, 1991.

986   36. Maraun, D.: Bias correction, quantile mapping, and downscaling: Revisiting the

987   inflation issue. J. Clim. 26(6), 2137-2143, https://doi.org/10.1175/JCLI-D-12-

988   00821.1, 2013.

989   37. Nair, M.M.A., Rajesh, N., Sahai, A.K., and Lakshmi Kumar, T.V.: Quantification of

990   uncertainties in projections of extreme daily precipitation simulated by CMIP6

991   GCMs over homogeneous regions of India. Int. J. Climatol. 43(15), 7365-7380,

992   https://doi.org/10.1002/joc.8269, 2023.

993   38. Nash, J.E., and Sutcliffe, J.V.: River flow forecasting through conceptual models part

994   I—A discussion of principles. J. Hydrol. 10**,** 282–290, https://doi.org/10.1016/0022-

995   1694(70)90255-6Return to ref 1970 in article, 1970.

996   39. Pathak, R., Dasari, H.P., Ashok, K., and Hoteit, I., Effects of multi-observations

997   uncertainty and models similarity on climate change projections. npj clim. atmos. sci.

998   6, 144, https://doi.org/10.1038/s41612-023-00473-5, 2023.

999   40. Piani, C., Weedon, G. P., Best, M., Gomes, S. M., Viterbo, P., Hagemann, S., and

1000   Haerter, J.O.: Statistical bias correction of global simulated daily precipitation and

1001   temperature for the application of hydrological models. J. Hydrol. 395(3-4), 199-215,

1002 https://doi.org/10.1016/j.jhydrol.2010.10.024, 2010.

41. Rahimi, R., Tavakol-Davani, H., and Nasseri, M.: An Uncertainty-Based Regional Comparative Analysis on the Performance of Different Bias Correction Methods in Statistical Downscaling of Precipitation. Water Resour. Manag. 35, 2503–2518, https://doi.org/10.1007/s11269-021-02844-0, 2021.

42. Rajulapati, C.R., and Papalexiou, S.M.: Precipitation Bias Correction: A Novel Semi-parametric Quantile Mapping Method. Earth Space Sci. 10(4), e2023EA002823, https://doi.org/10.1029/2023EA002823, 2023.

43. Saranya, M.S., and Vinish, V.N.: Evaluation and selection of CORDEX-SA datasets and bias correction methods for a hydrological impact study in a humid tropical river basin, Kerala. Water Climate Change 12(8), 3688-3713, https://doi.org/10.2166/wcc.2021.139, 2021.

44. Shanmugam, M., Lim, S., Hosan, M.L. Shrestha, S., Babel, M.S., and Virdis, S.G.P.: Lapse rate-adjusted bias correction for CMIP6 GCM precipitation data: An application to the Monsoon Asia Region. Environ Monit Assess. 196, 49, https://doi.org/10.1007/s10661-023-12187-5, 2024.

45. Smitha, P.S., Narasimhan, B., Sudheer K.P., and Annamalai, H.: An improved bias correction method of daily rainfall data using a sliding window technique for climate change impact assessment. J. Hydrol. 556, 100-118. https://doi.org/10.1016/j.jhydrol.2017.11.010, 2018

46. Song, J. Y., and Chung, E.S.: Robustness, uncertainty, and sensitivity analyses of TOPSIS method to climate change vulnerability: Case of flood damage. Water Resour. Manag., 30(13), 4751–4771, https://doi.org/10.1007/s11269-016-1451-2, 2016.

47. Song, Y.H., Shahid, S., and Chung, E.S.: Differences in multi-model ensembles of CMIP5 and CMIP6 projections for future droughts in South Korea. Int. J. Climatol. 42(5), 2688-2716, https://doi.org/10.1002/joc.7386, 2022a.

48. Song, Y.H., Chung, E.S., and Shahid, S.: The New Bias Correction Method for Daily Extremes Precipitation over South Korea using CMIP6 GCMs. Water Resour. Manag. 36, 5977–5997, https://doi.org/10.1007/s11269-022-03338-3, 2022b.

49. Song, Y.H., Chung, E.S., and Shahid, S.: Uncertainties in evapotranspiration projections associated with estimation methods and CMIP6 GCMs for South Korea.

1034   Sci. Total Environ. 825, 153953, https://doi.org/10.1016/j.scitotenv.2022.153953,
1035   2023.

1036 50. Song, Y.H., Chung, E.S., and Shahid, S.: Global Future Climate Signal by Latitudes
1037   Using CMIP6 GCMs. Earths Future 12(3), e2022EF003183,
1038   https://doi.org/10.1029/2022EF003183, 2024a.

1039 51. Song, Y.H.: Comprehensive Index and Performance-Related Code, Zenodo [Code],
1040   https://zenodo.org/records/14351816. 2024b

1041 52. Song, Y.H.: Historical Daily Precipitation Data of CMIP6 GCMs and ERA5,
1042   Figshare [Dataset], https://doi.org/10.6084/m9.figshare.27999167.v5. 2024c

1043 53. Switanek, M.B., Troch, P.A., Castro, C.L., Leuprecht, A., Chang, H.I, Mukherjee,
1044   R., and Demaria E.M.C.: Scaled distribution mapping: a bias correction method that
1045   preserves raw climate model projected changes. HESS 21(6), 2649-2666,
1046   https://doi.org/10.5194/hess-21-2649-2017, 2017.

1047 54. Tanimu, B., Bello, AA.D., Abdullahi, S.A. Ajibike, M.A., Yaseen, Z.M.,
1048   Kamruzzaman, M., Muhammad, M.K.I., and Shahid, S.: Comparison of conventional
1049   and machine learning methods for bias correcting CMIP6 rainfall and temperature in
1050   Nigeria. Theor. Appl. Climatol. 155, 4423–4452, https://doi.org/10.1007/s00704-
1051   024-04888-9, 2024.

1052 55. Teutschbein, C., and Seibert, J.: Bias correction of regional climate model
1053   simulations for 575 hydrological climate-change impact studies: Review and
1054   evaluation of different 576 methods. J. Hydrol. 16, 12-29,
1055   http://dx.doi.org/10.1016/j.jhydrol.2012.05.052, 2012.

1056 56. Teng, J., Potter, N. J., Chiew, F. H. S., Zhang, L., Wang, B., Vaze, J., and Evans,
1057   J.P.: 2015. How does bias correction of regional climate model precipitation affect
1058   modelled runoff? HESS 19, 711–728, https://doi.org/10.5194/hess-19-711-2015,
1059   2015.

1060 57. Themeßl, M.J., Gobiet, A., and Heinrich, G.: Empirical-statistical downscaling and
1061   error correction of daily precipitation from regional climate models. Int. J. Climatol.
1062   31(10), 1530-1544, https://doi.org/10.1002/joc.2168, 2012.

1063 58. Tong, Y., Gao, X., Han, Z., Xu, Y., and Giorgi, F.: Bias correction of temperature
1064   and precipitation over China for RCM simulations using the QM and QDM methods.
1065   Clim. Dyn. 57, 1425-1443, https://doi.org/10.1007/s00382-020-05447-4, 2021.

1066   59. Yip, S., Ferro, C.A.T., Stephenson, D.B., and Hawkins, E.: A simple, coherent
1067   framework for partitioning uncertainty in climate predictions. J. Clim. 24(17), 4634–
1068   4643, https://doi.org/10.1175/2011JCLI4085.1, 2011.

1069   60. Woldemeskel, F. M., Sharma, A. Sivakumar, B., and Mehrotra, R.: A framework to
1070   quantify GCM uncertainties for use in impact assessment studies. J. Clim. 519,
1071   1453–1465, https://doi.org/10.1016/j.jhydrol.2014.09.025, 2014.

1072   61. Wu, Y., Miao, C., Fan, X., Gou, J., Zhang, Q., and Zheng, H.: Quantifying the
1073   uncertainty sources of future climate projections and narrowing uncertainties with
1074   Bias Correction Techniques. Earths Future, 10(11), e2022EF002963, 2022.

1075   62. Zhang, S., Zhou, Z., Peng, P., and Xu, C.: A New Framework for Estimating and
1076   Decomposing the Uncertainty of Climate Projections. J. Clim. 37(2), 365-384,
1077   https://doi.org/10.1175/JCLI-D-23-0064.1, 2024.

1078